Supporting Information.

# 1D Zn(II)/2D Cu(I) halogen pyridyl coordination polymers. Band gap engineering by DFT for predicting more efficient photocatalysts in water treatment.

Andrea García-Hernán[α], Fernando Aguilar-Galindo[γ,δ], Oscar Castillo[χ], Pilar Amo-Ochoa[α,δ]*

[α]*Dpto. de Química Inorgánica. Universidad Autónoma de Madrid, 28049 Madrid, Spain.*

[γ]*Dpto. Química Universidad Autónoma de Madrid, 28049 Madrid, Spain*

[δ]*Institute for Advanced Research in Chemical Sciences (IAdChem). Universidad Autónoma de Madrid, 28049 Madrid, Spain*

[χ]*Department of Organic and Inorganic Chemistry, University of the Basque Country UPV/EHU, 48080 Bilbao, Spain*

E-mail: pilar.amo@uam.es

## 1. Experimental details

### 1.1 Synthesis and characterization of $[ZnX_2(L)]_n$ compounds (L=BPE, and BPEE, X= Cl, Br, and I)

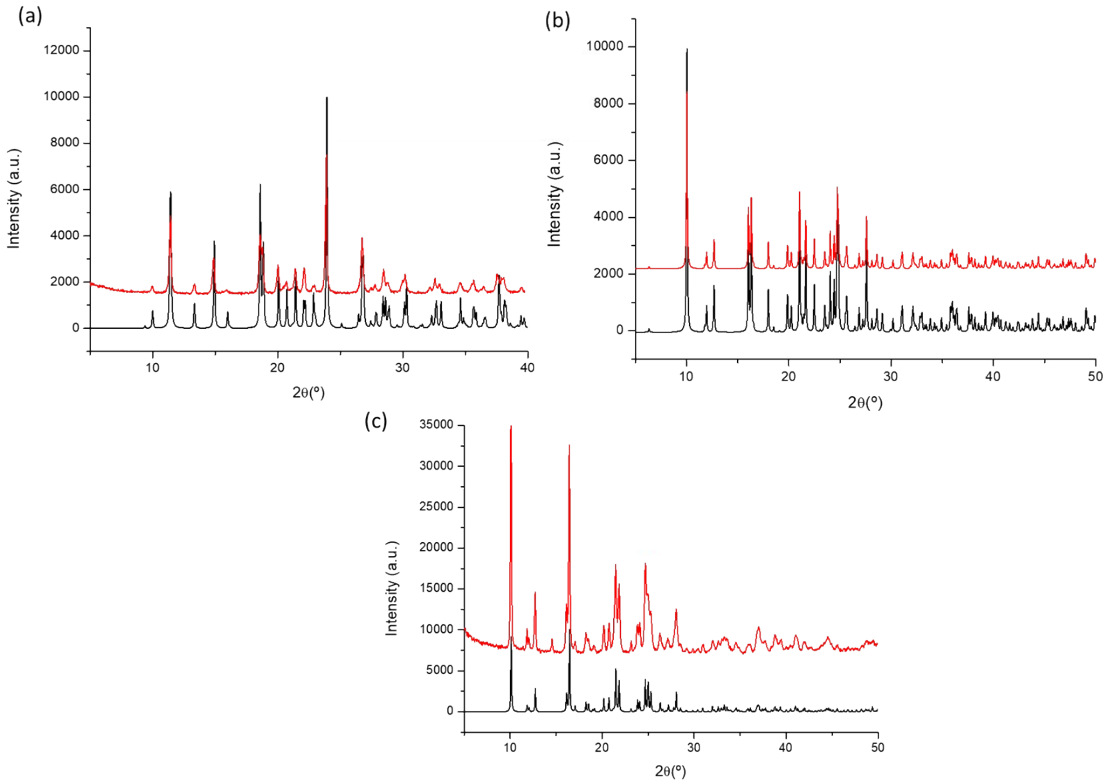


**Figure S1**: P-XRD of compounds: (a) **3a,** b) **2a** and c) **1a**. P-XRD simulated (black) and experimental (red).

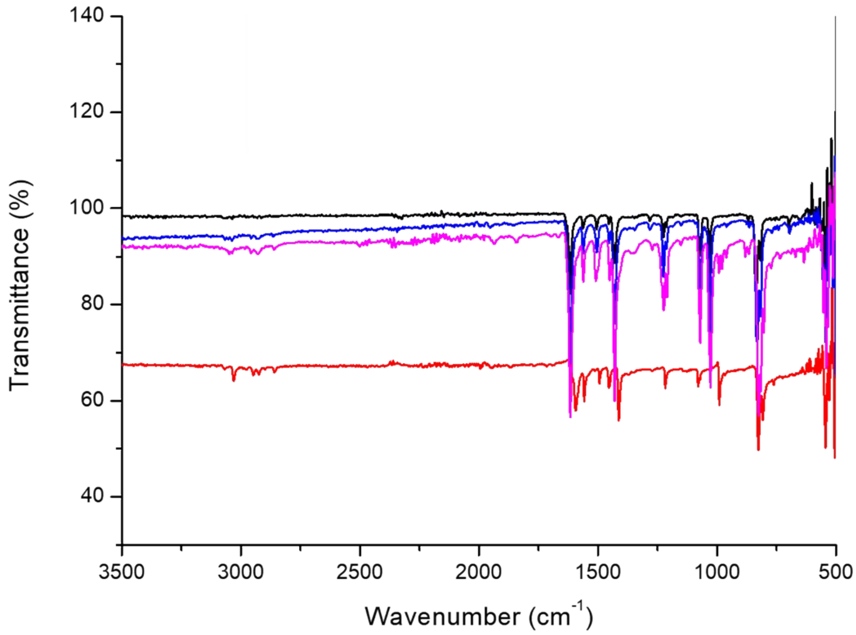


**Figure S2**: Infrared spectrum of compounds: **3a**, pink; **2a**, blue; **1a**, black; and the BPE ligand, red.

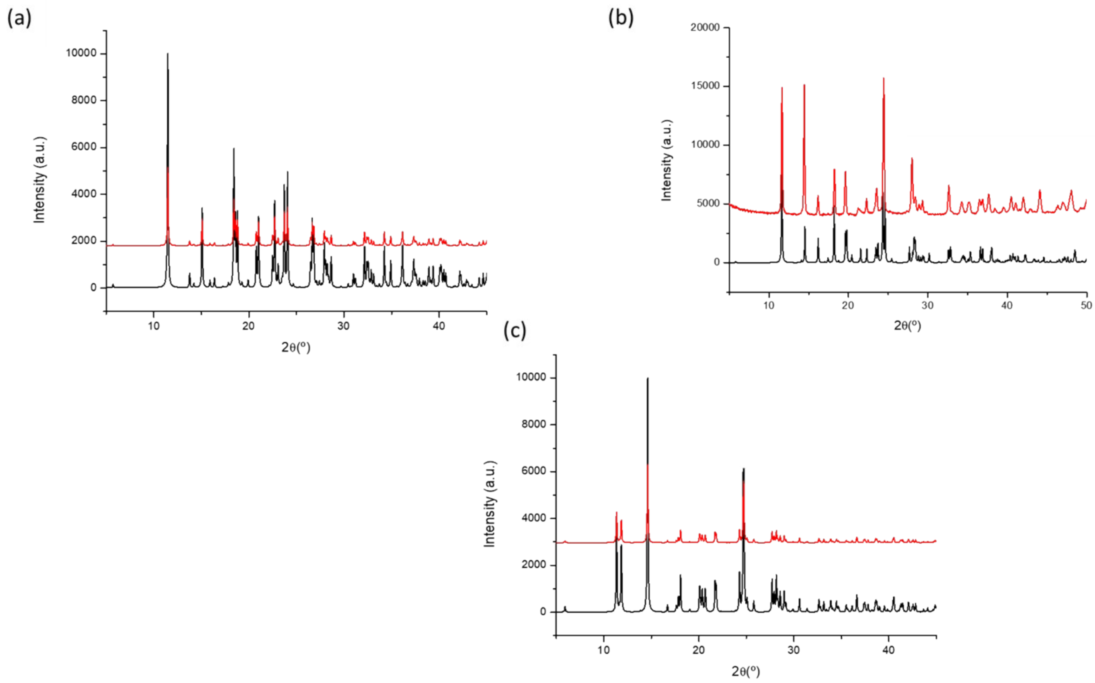


**Figure S3**: P-XRD of compounds (a) **3b**, (b) **2b** and (c) **1b.** P-XRD Simulated (black) and experimental (red).

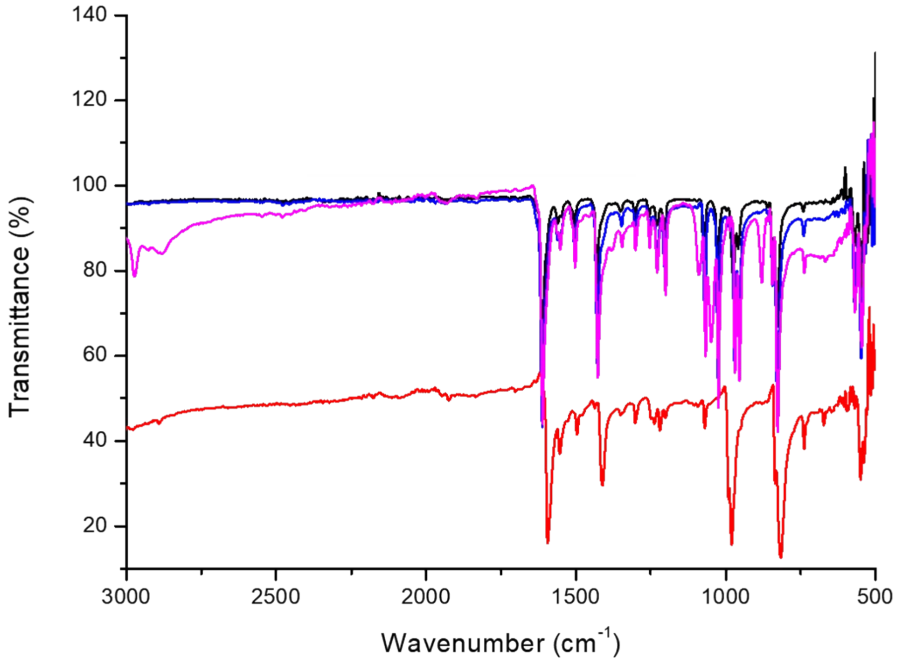


**Figure S4**: Infrared spectrum of compounds **3b**, pink; **2b**, blue; **1b**, black, and BPEE ligand, red.

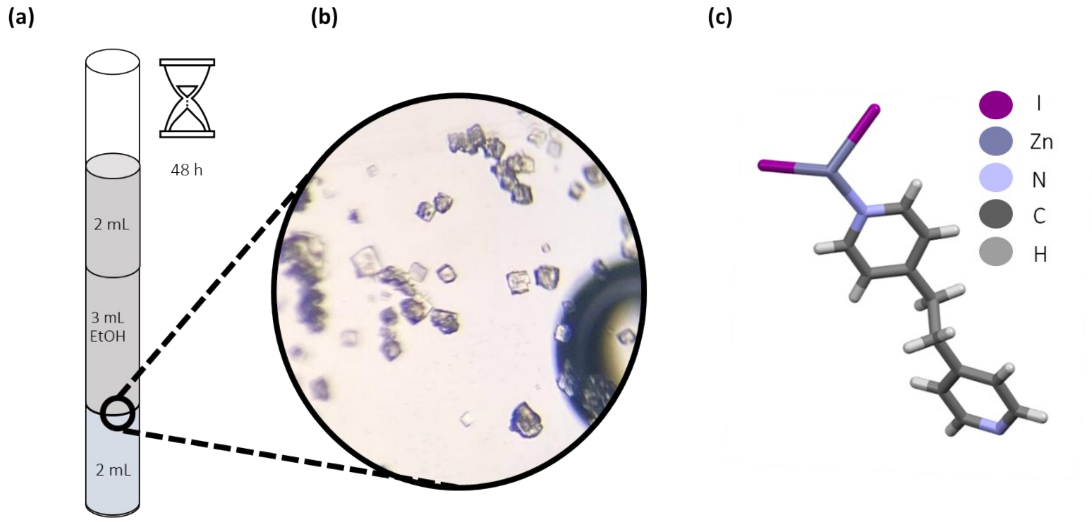


**Figure S5**. Crystallization scheme of **3a**: a) The two reagents, BPE in EtOH (gray) and $ZnI_2$ in water (blue), overlap by dropwise addition inside a test tube where there is an EtOH intermedium to slow down the reaction between the reactants, b) Optical imagen of single crystals of **3a** and c) asymmetric unit of **3a.**

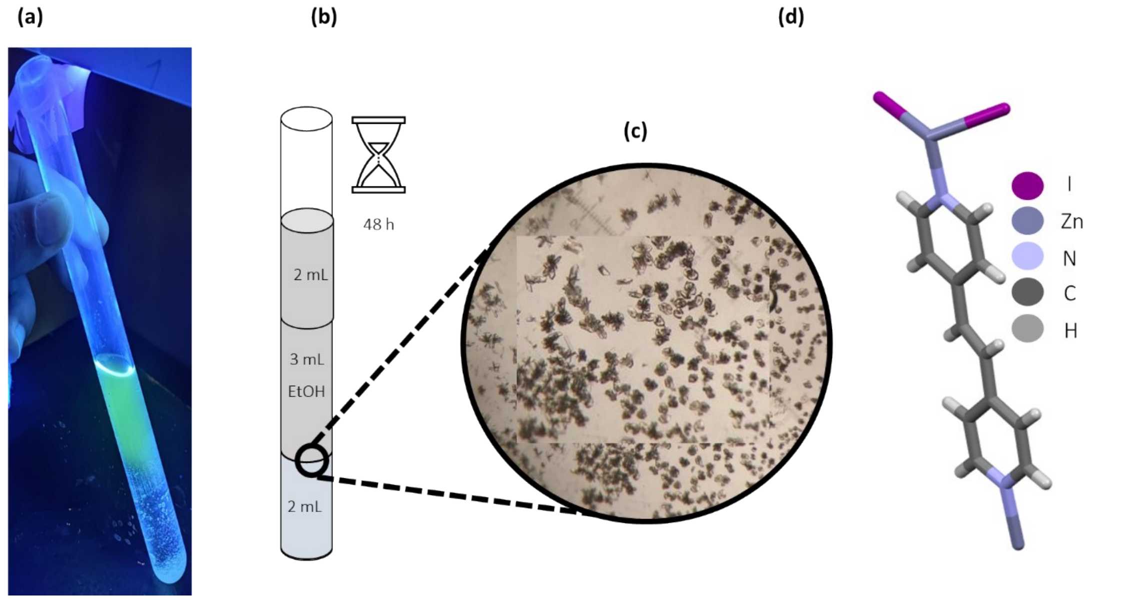


**Figure S6**. a) test tube under UV light (λ=365 nm); b) crystallization scheme of **3b**. The two reagents, BPEE in EtOH (gray) and $ZnI_2$ in water (blue), overlap by dropwise addition inside a test tube where there is an EtOH intermedium to slow down the reaction between the reactants, c) Optical image of single crystals of **3b** and d) asymmetric unit of **3b**.

## 1.2. Synthesis and characterization of $[Cu_2X_2(BPEE)]_n$ compounds (X=Cl, Br, and I).

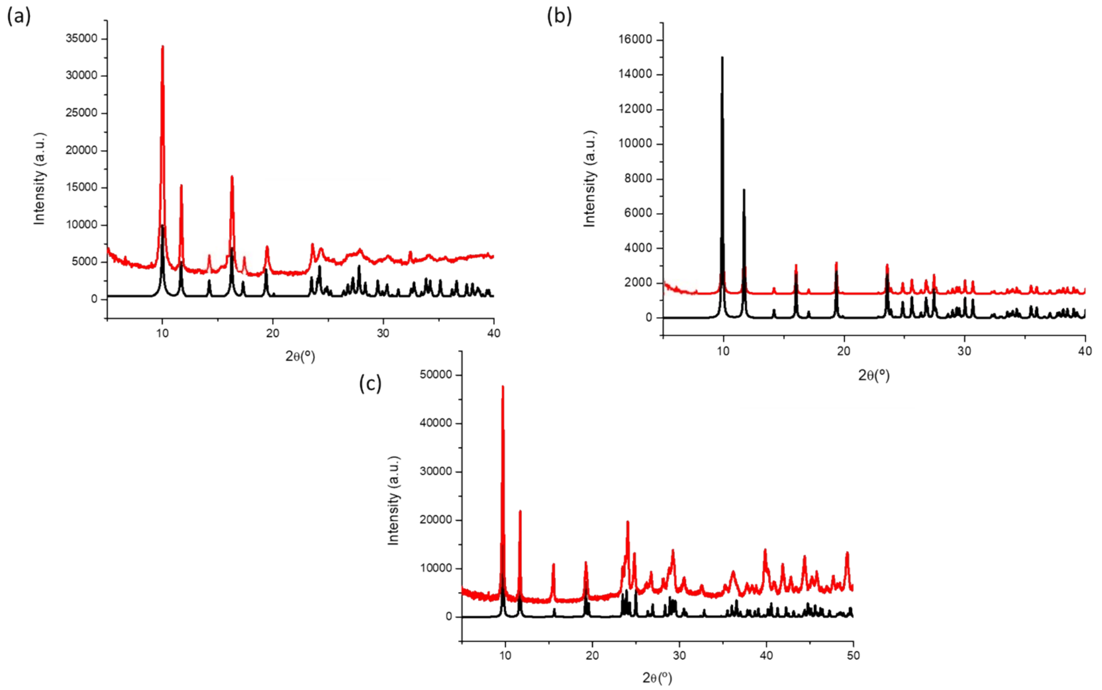


**Figure S7**: P-XRD of compounds (a) **4b**, ( b) **5b** and (c) **6b**. P-XRD Simulated (black) and experimental (red).

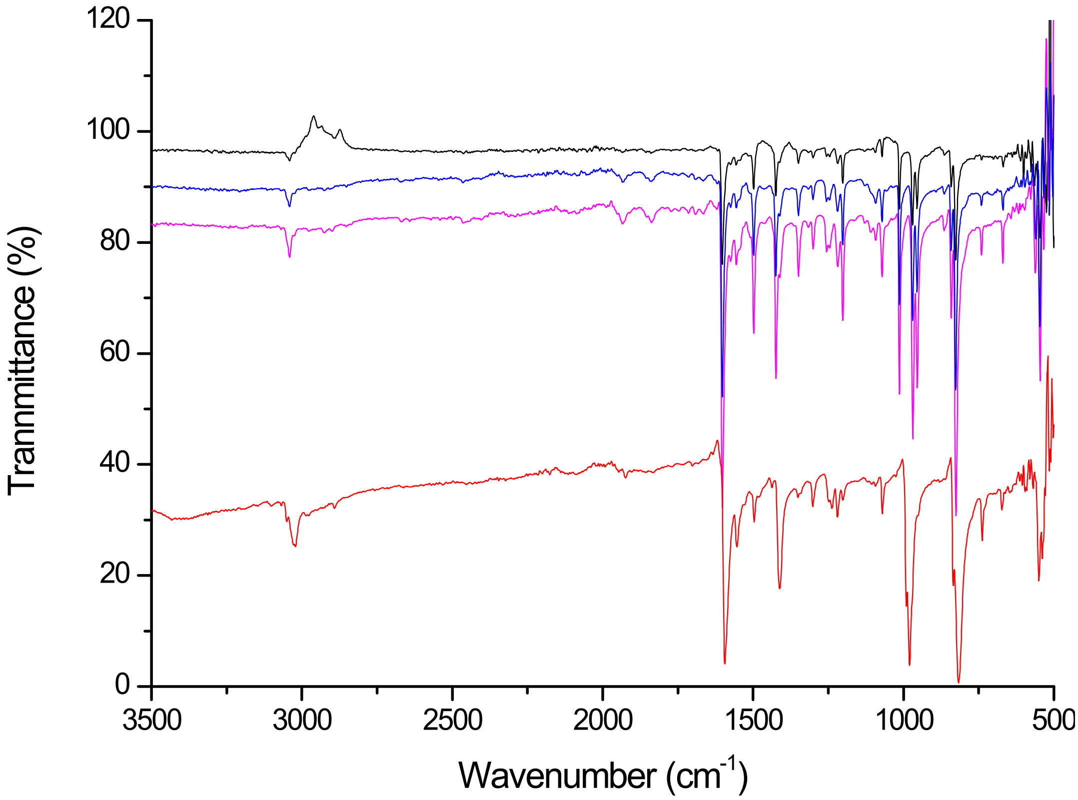


**Figure S8**: Infrared spectrum of compounds **6b**, pink; **5b**, blue; **4b**, black, and BPEE ligand in red.

**2. DFT calculations to explore $[ZnX_2(BPE)]_n$ (X=Cl (1a), Br (2a), and I (3a)) theoretical band gaps and correlation with the experimental ones.**

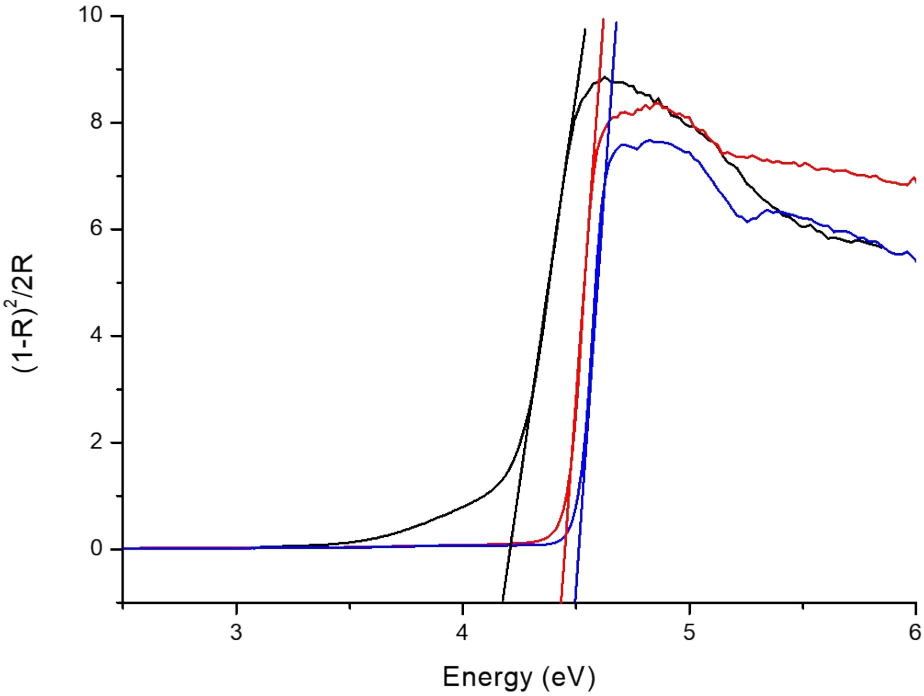


**Figure S9_** Experimental Band gap values by diffuse reflectance: **3a** (black), **2a** (red), and **1a** (blue).

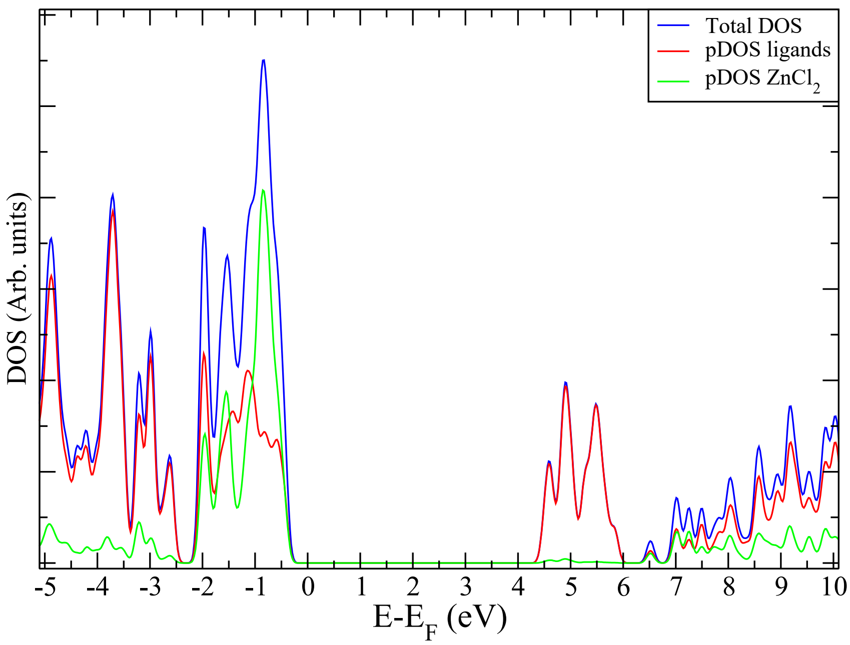


**Figure S10.** Density of States of **1a** and projection on the atoms of ligands and on the atoms of the $ZnCl_2$ unit.

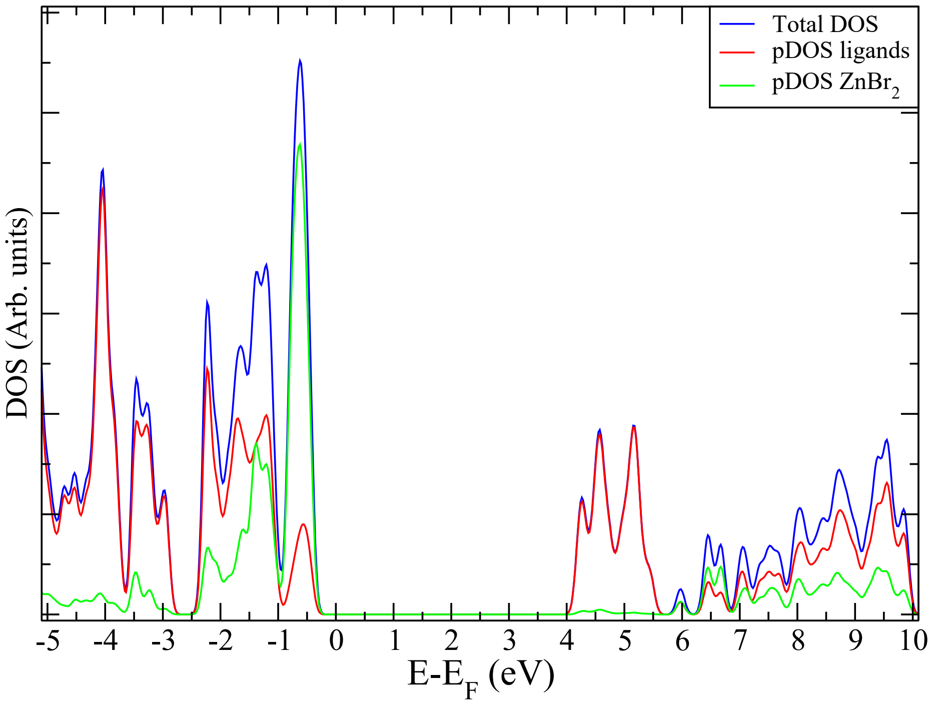


**Figure S11:** Density of States of **2a** and projection on the atoms of ligands and on the atoms of the $ZnBr_2$ unit.

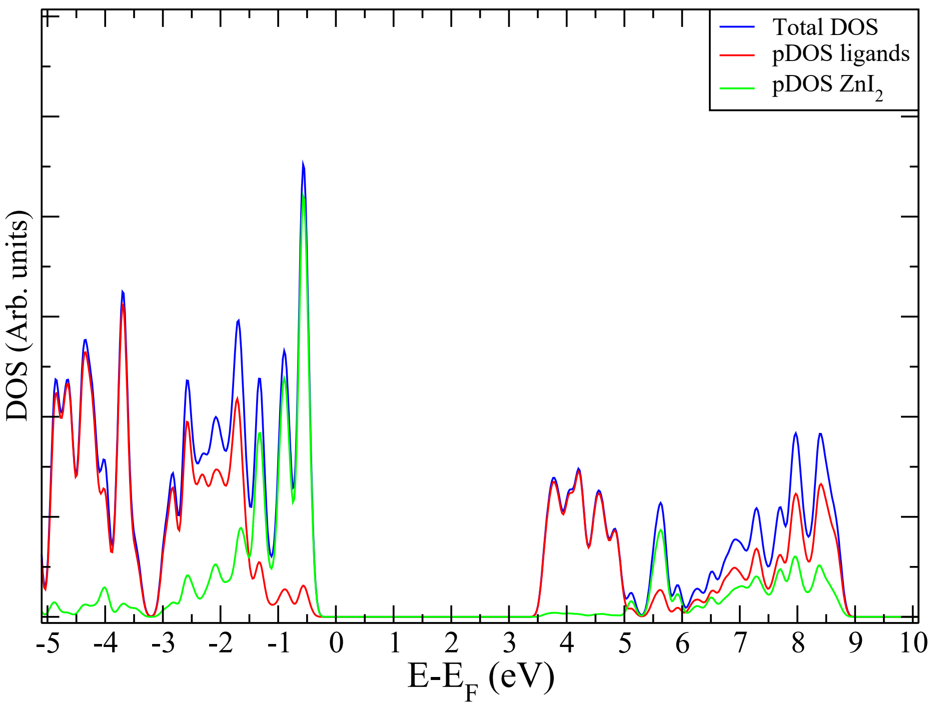


**Figure S12**: Density of States of **3a** and projection on the atoms of ligands and the atoms of the $ZnI_2$ unit.

**Table S1.** Atomic charges of the Zn, the halogen, and the nitrogen on the $[ZnX_2(BPE)]_n$ (X= Cl (**1a**), Br (**2a**), and I (**3a**)) compounds.

| Atom | **1a** | **2a** | **3a** |
|---|---|---|---|
| Zn | 1.20 | 1.12 | 1.02 |
| X | -0.70 | -0.64 | -0.57 |
| N | -1.32 | -1.34 | -1.34 |

**3. Calculation of Atomic Economy (AE) and E-factor in $[ZnX_2(BPE)]_n$, $[ZnX_2(BPEE)]_n$ and $[Cu_2X_2(BPEE)]_n$ (X=Cl, Br, and I) compounds using the optimizing methodologies employing environmentally friendly procedures.**

**Table S2.** E-Factor and AE in CPs

| | **1a** | **2a** | **3a** | **1b** | **2b** | **3b** | **4b** | **5b** | **6b** | **4b*** | **5b*** | **6b*** |
|---|---|---|---|---|---|---|---|---|---|---|---|---|
| **E-factor** | 0,17 | 0,08 | 0,02 | 0,09 | 0,05 | 0,05 | 0,21 | 0,02 | 0,02 | *1.98* | *1.16* | *1.12* |
| **AE** | 0,77 | 0,85 | 0,87 | 0,78 | 0,84 | 0,83 | 0,86 | 0,9 | 0,84 | *0.33* | *0.46* | *0.36* |

*Previously reported

**4. DFT calculations to explore $[ZnX_2(BPEE)]_n$ (X=Cl (1b), Br (2b), and I (3b)) theoretical band gaps and correlation with the experimental ones.**

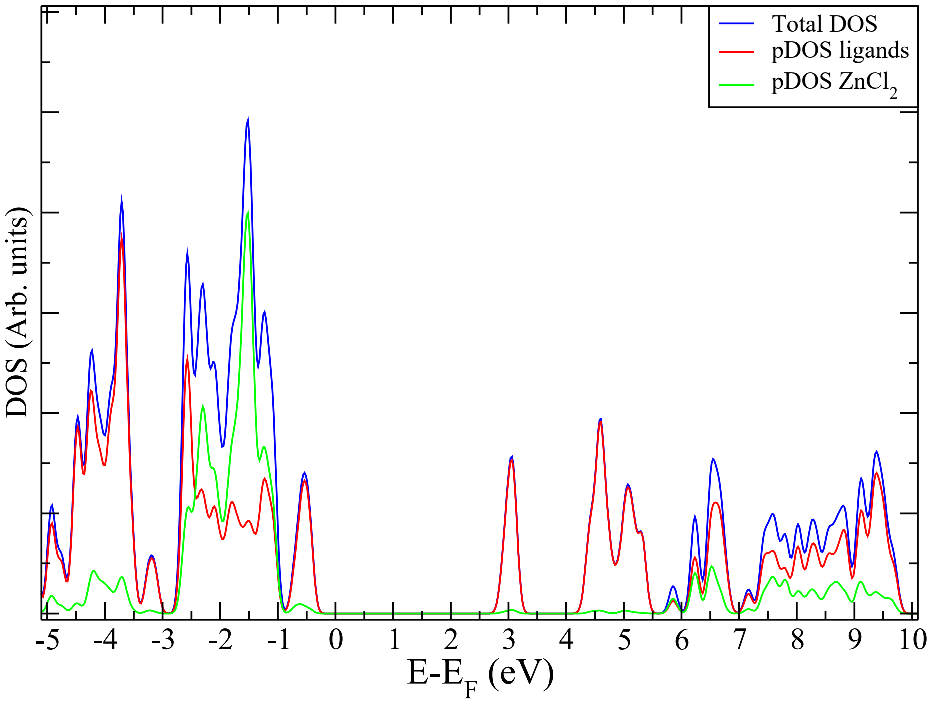


**Figure S13**: Density of States of **1b**, and projection on the atoms of ligands and on the atoms of the $ZnCl_2$ unit.

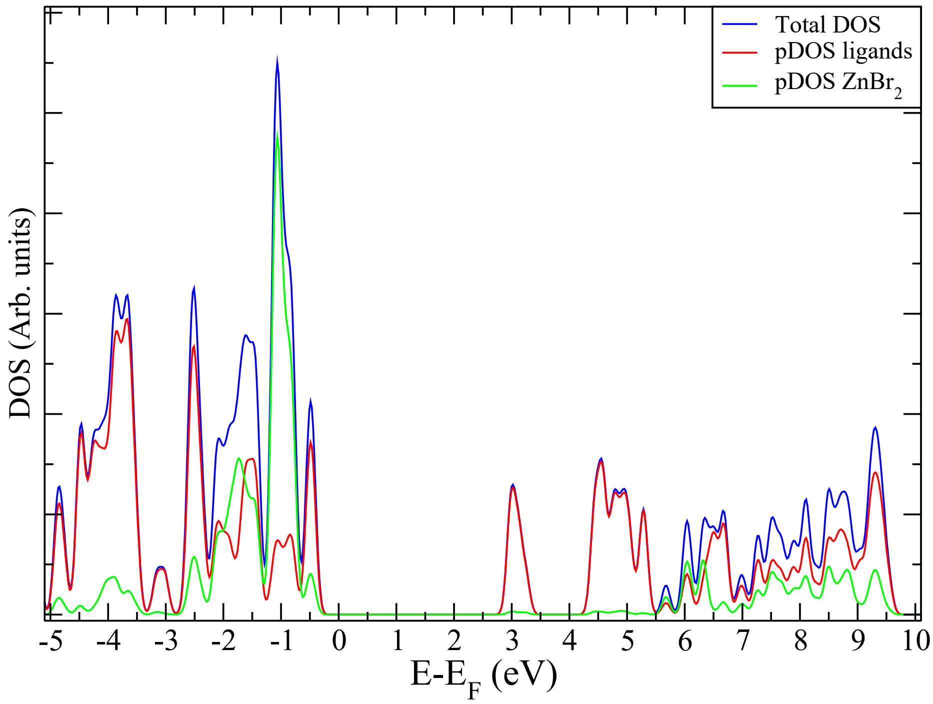


**Figure S14**: Density of States of **2b**, and projection on the atoms of ligands and on the atoms of the $ZnBr_2$ unit.

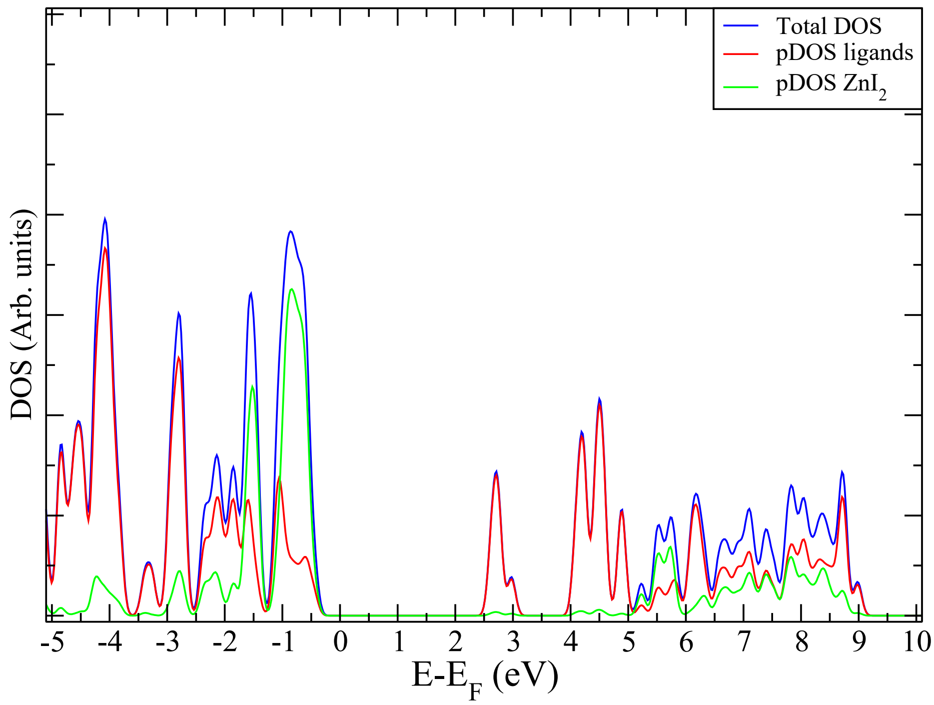


**Figure S15**: Density of States of **3b**, and projection on the atoms of ligands and on the atoms of the $ZnI_2$ unit.

**Table S3**: Atomic charges of the Zn, the halogen, and the nitrogen on the $[ZnX_2(BPEE)]_n$ (X=Cl (**1b**), Br (**2b**), and I (**3b**)) compounds.

| Atom | **1b** | **2b** | **3b** |
|---|---|---|---|
| Zn | 1.20 | 1.12 | 1.02 |
| X | -0.70 | -0.64 | -0.56 |
| N | -1.35 | -1.33 | -1.34 |

## 5. Study of the particle size of $[ZnX_2(BPEE)]_n$ (X=Cl (1b), Br (2b), and I (3b)) compounds

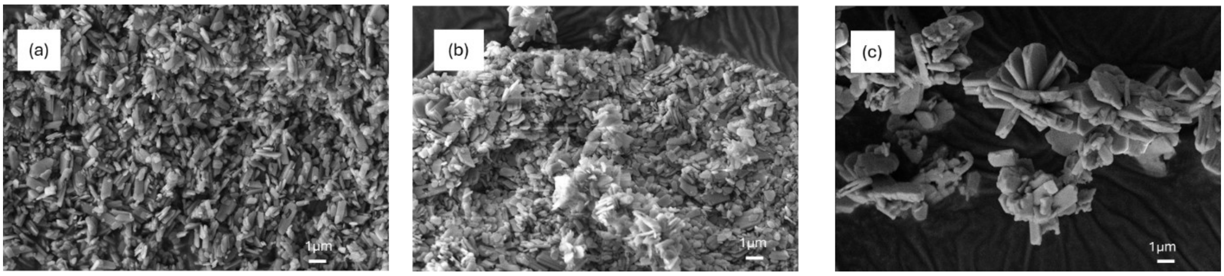


**Figure S16:** SEM images of the compounds: (a) **1b**, (b) **2b**, and (c) **3b**.

**Table S4:** Particle size of **$[ZnX_2(BPEE)]_n$** (X=Cl (**1b**), Br (**2b**), and I (**3b**)) measured on 50 particles

| | **1b** | **2b** | **3b** |
|---|---|---|---|
| Size (μm) length | 0.9 ± 0,5 | 0.8 ± 0,3 | 2.5 ± 0.7 |
| Size (μm) width | 0.4 ± 0,2 | 0.7 ± 0,4 | 0.9 ± 0,4 |

## 6. Crystallographic data and structure analysis.

**Table S5:** Crystallographic data and structure refinement details of **3a**, and **3b** compounds.[a,b]

| | **3a** | **3b** |
|---|---|---|
| empirical formula | $C_{12}H_{12}I_2N_2Zn$ | $C_{12}H_{10}I_2N_2Zn$ |
| formula weight | 503.41 | 501.39 |
| crystal system | Monoclinic | Triclinic |
| space group | *C*2/*c* (15) | *P*-1 (2) |
| *a* | 16.3937(5) | 5.8775(2) |
| *b* | 11.8607(3) | 8.0332(2) |
| c | 16.2836(4) | 15.8128(4) |
| α | 90 | 102.779(2) |
| β | 108.595(3) | 91.996(2) |
| γ | 90 | 91.958(2) |
| V (Å$^3$) | 3000.91(15) | 727.00(4) |
| Z | 8 | 2 |
| T (K) | 200.0(1) | 298(1) |
| λ (Å) | 1.54184 | 0.71073 |
| Sizes (mm) | 0.12/0.07/0.02 | 0.25/0.10/0.01 |
| Shape | Prism | Prism |

| | | |
|---|---|---|
| Color | Colorless | Colorless |
| Max. and medium Δ/σ | 0.001/0.000 | 0.001/0.000 |
| θ interval | 4.690 – 68.326 | 2.602 – 25.364 |
| hkl interval | $-19 \leq h \leq 19$<br>$-13 \leq k \leq 14$<br>$-19 \leq l \leq 19$ | $-7 \leq h \leq 7$<br>$-9 \leq k \leq 9$<br>$-18 \leq l \leq 19$ |
| $\rho_c$ (g·cm$^{-3}$) | 2.228 | 2.290 |
| $\mu$ (cm$^{-1}$) | 34.422 | 5.916 |
| $F$(000) | 1872 | 464 |
| S$^a$ | 1.040 | 1.063 |
| $R_{int}$ | 0.0414 | 0.0446 |
| Parameters | 154 | 154 |
| Weight scheme$^c$ | Shelx | Shelx |
| final R indices | | |
| [I > 2σ(I)] $R_1^b/wR_2^c$ | 0.0323/0.0870 | 0.0271/0.0614 |
| all data $R_1^b/wR_2^c$ | 0.0345/0.0887 | 0.0331/0.0641 |

$^a S=[\sum w(F_0^2-F_c^2)^2/(N_{obs}-N_{param})]^{1/2}$. $^b R_1=\sum||F_0|-|F_c||/\sum|F_0|$. $^c wR_2 = [\sum w(F_0^2-F_c^2)^2/\sum wF_0^2]^{1/2}$; $w = 1/[\sigma^2(F_0^2) + (aP)^2 + b]$ where $P = (\max(F_0^2,0) + 2F_c^2)/3$; $[ZnI_2(BPE)]_n$ (a = 0.0630, b = 2.1271) and $[ZnI_2(BPEE)]_n$ (a = 0.0256, b = 0.4052).

**Table S6:** Selected bond lengths (Å) and angles (º) for compounds **3a**, and **3b**.[a]

| | **3a** | **3b** |
|---|---|---|

| | | |
|---|---|---|
| Zn1-I1 | 2.5884(5) | 2.5430(5) |
| Zn1-I2 | 2.5526(5) | 2.5891(6) |
| Zn1-N1 | 2.048(3) | 2.064(3) |
| Zn1-N2 | 2.056(3)$^{i}$ | 2.065(3) |
| Zn1···Zn1 | 13.3735(8)$^{ii}$ | 13.4718(10)$^{iii}$ |
| I1-Zn1-I2 | 121.62(2) | 124.69(2) |
| I1-Zn1-N1 | 107.09(9) | 108.69(10) |
| I1-Zn1-N2 | 107.90(9)$^{i}$ | 109.17(10) |
| I2-Zn1-N1 | 108.04(9) | 104.09(10) |
| I2-Zn1-N2 | 107.30(9)$^{i}$ | 103.46(10) |
| N1-Zn1-N2 | 103.45(14)$^{i}$ | 105.12(14) |

aSymmetry codes: (i) x+1/2, -y+1/2, z+1/2; (ii) x-1/2, -y+1/2, z-1/2; (iii) -x+2, -y+1, -z+2.

**Table S7:** Hydrogen bonding interactions in compounds **3a**, and **3b**.[a]

| **3a** | | | |
|---|---|---|---|
| D–H...Ab | H...A | D...A | D–H...A |
| C11–H11...I1[i] | 3.09 | 3.767(4) | 129.9 |
| C5–H5...I1 | 3.16 | 3.806(4) | 126.6 |
| C4-H4···I2[ii] | 3.31 | 4.094(4) | 141.5 |
| C10-H10···I1[iii] | 3.28 | 3.900(4) | 124.9 |
| C2–H2...I1[iv] | 3.29 | 4.217(4) | 165.1 |
| **3b** | | | |
| D–H...Ab | H...A | D...A | D–H...A |
| C1 H1 I1 | 3.26 | 3.873(4) | 125.3 |
| C4 H4 I2[i] | 3.29 | 4.021(5) | 137.2 |
| C5 H5 I2 | 3.26 | 3.799(5) | 119.1 |
| C7 H7 I1 | 3.28 | 3.888(4) | 124.7 |
| C11 H11 I2 | 3.19 | 3.758(4) | 121.6 |

[a]Symmetry codes for **3a**: (i) x-1/2, -y+1/2, z-1/2; (ii) x, -y+1, z-1/2; (iii) 5_666 -x+1, -y+1, -z+1; (iv) x-1/2, y-1/2, z. Symmetry codes for **3b**: (i) 2_677 -x+1, -y+2, -z+2.

b D = donor; A = acceptor.

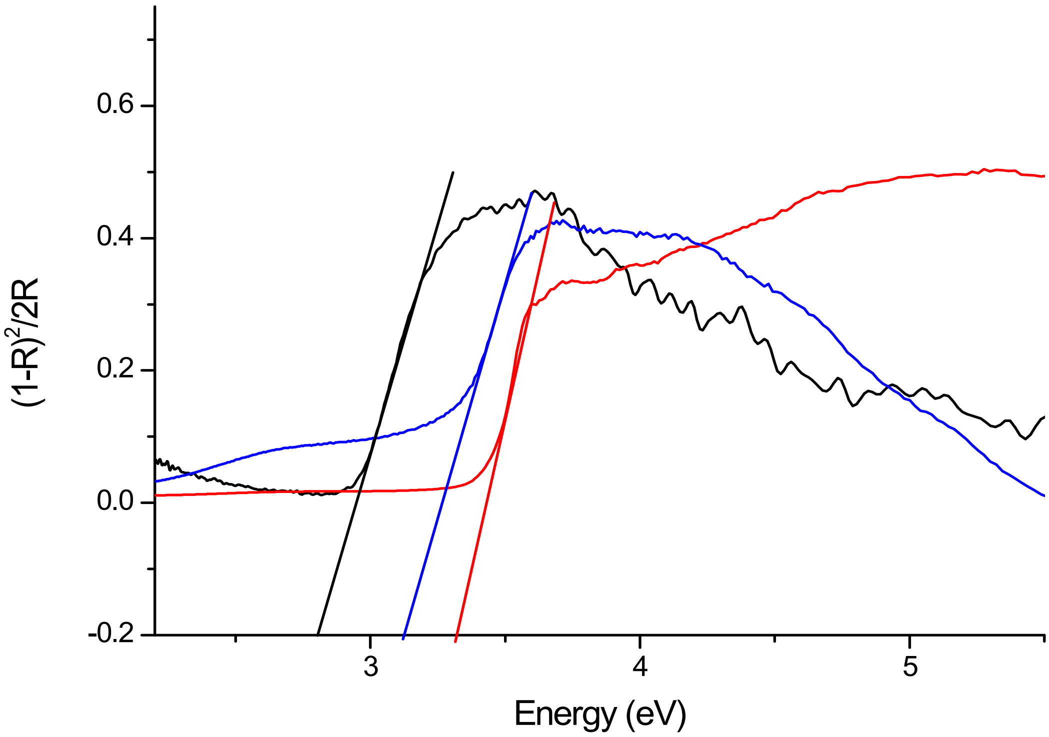


**Figure S17**. Band gap experimental value by diffuse reflectance: **1b**, black, **2b** red, and **3b**, blue.

### 7. Analysis of the coordination bonds distances distribution.

Coordination bond distribution found in the CSD database for $ZnX_2N_2$ (X = Cl, Br, and I) coordination environments in which the actual coordination bond distances of $[ZnX_2(BPE)]_n$ and $[ZnX_2(BPEE)]_n$ have been included as vertical lines. The color code is indicated in the graph. The vertical white line corresponds to the median value.

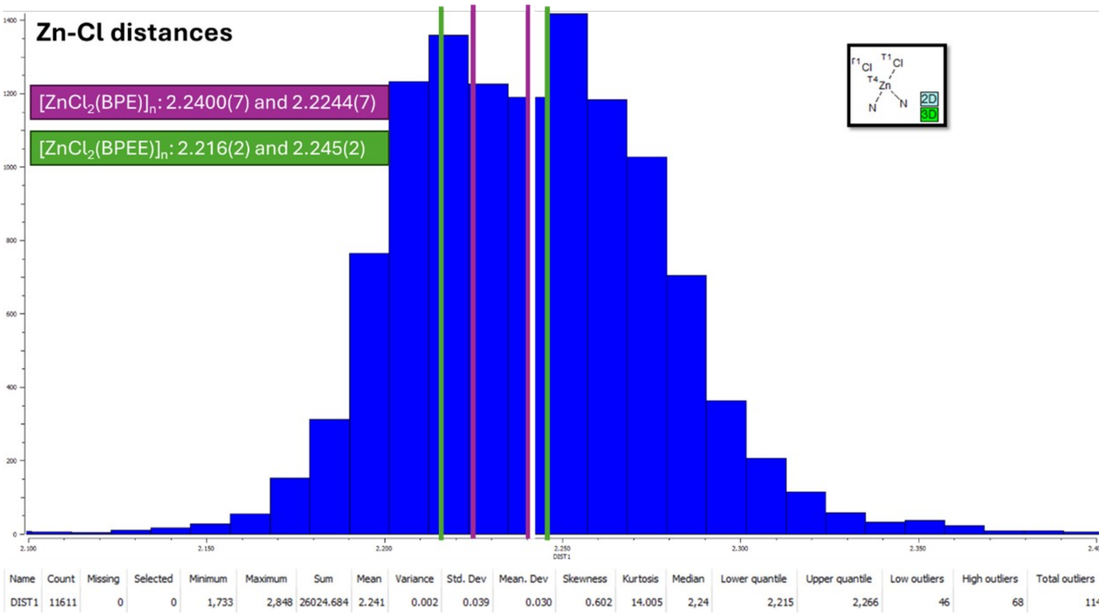


**Figure S18:** Zn-Cl coordination bond distances found in compounds: (a) **[ZnCl$_2$(BPE)]$_n$** and **[ZnCl$_2$(BPEE)]$_n$** placed within the distribution found in the CSD database for analogous $ZnCl_2N_2$ coordination environments.

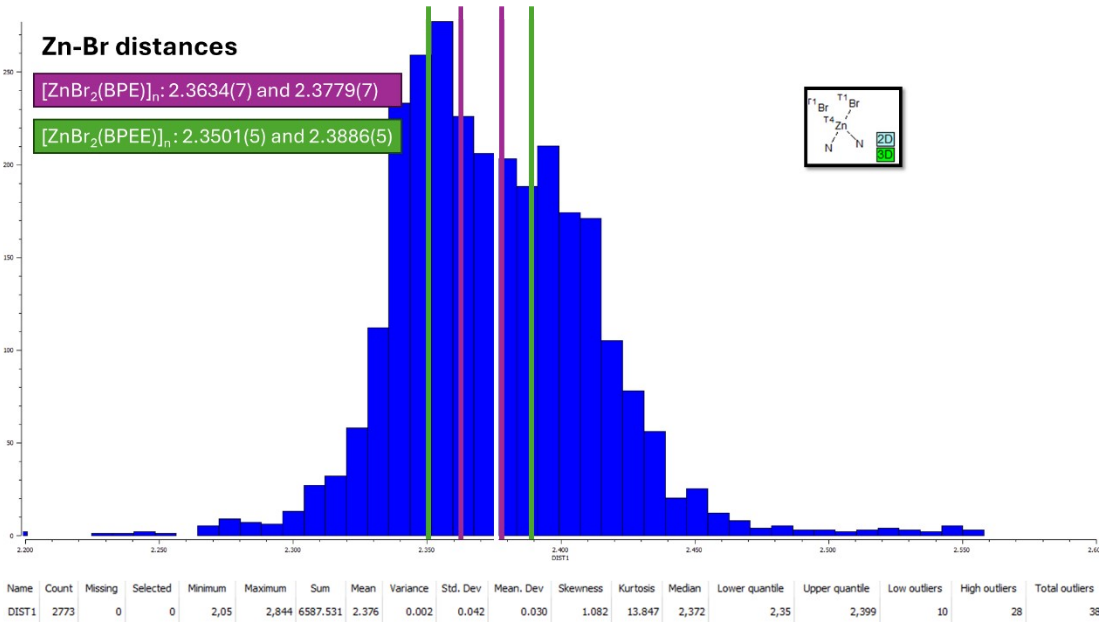


**Figure S19:** Zn-Br coordination bond distances found in compounds: (a) **[ZnBr$_2$(BPE)]$_n$** and **[ZnBr$_2$(BPEE)]$_n$** placed within the distribution found in the CSD database for analogous $ZnBr_2N_2$ coordination environments.

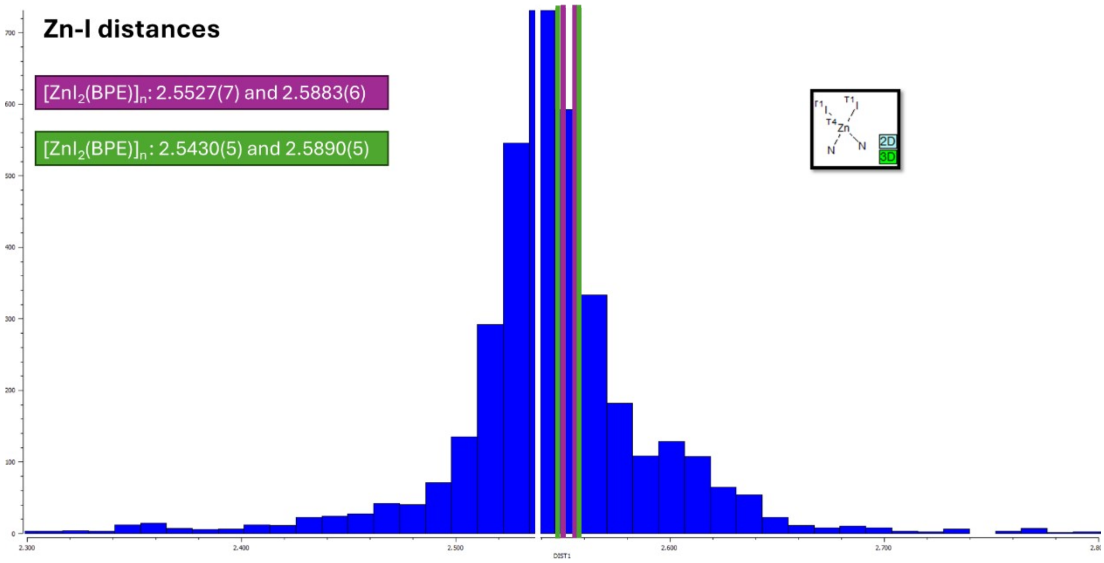


| Name | Count | Missing | Selected | Minimum | Maximum | Sum | Mean | Variance | Std. Dev | Mean. Dev | Skewness | Kurtosis | Median | Lower quantile | Upper quantile | Low outliers | High outliers | Total outliers |
|---|---|---|---|---|---|---|---|---|---|---|---|---|---|---|---|---|---|---|
| DIST1 | 3677 | 0 | 0 | 2,087 | 3,296 | 9361.629 | 2.546 | 0.003 | 0.056 | 0.033 | 1.002 | 21.149 | 2,544 | 2,527 | 2,563 | 52 | 32 | 8 |

**Figure S20:** Zn-I coordination bond distances found in compounds: (a) **$[ZnI_2(BPE)]_n$** and **$[ZnI_2(BPEE)]_n$** placed within the distribution found in the CSD database for analogous $ZnI_2N_2$ coordination environments.

8. **Water and thermal stability of $[ZnX_2(BPEE)]_n$ .**

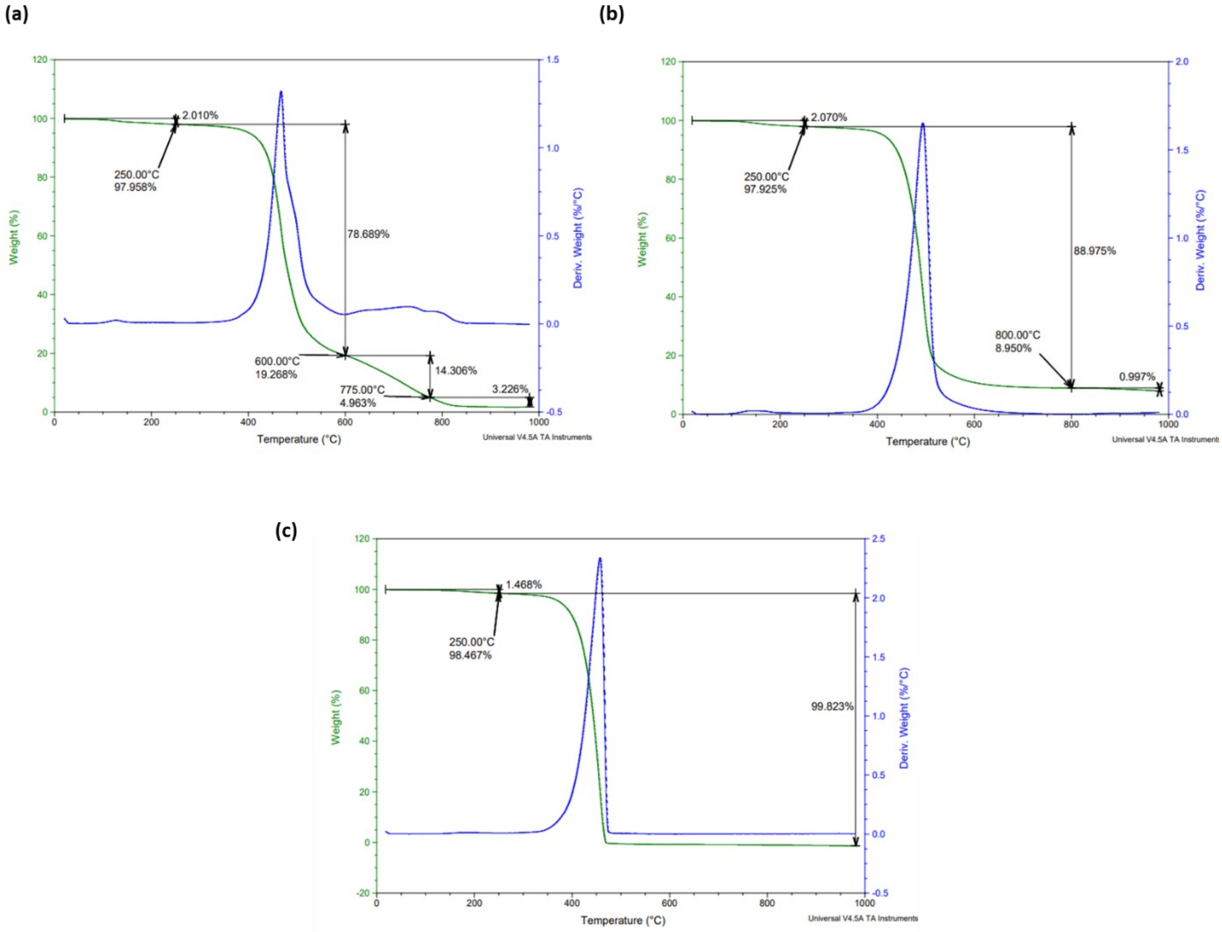


**Figure S21:** Thermogravimetric analysis (TGA) of the compounds: a) **1b**, b) **2b** and c) **3b.**

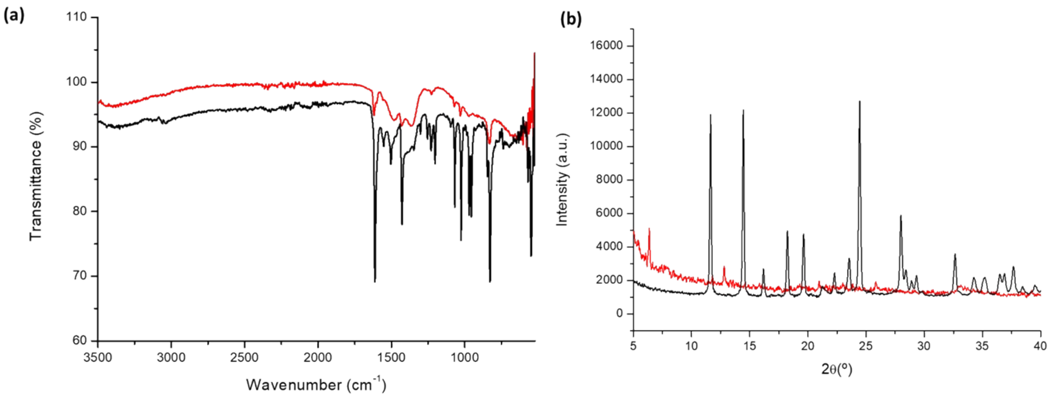

**Figure S22**: Example of water behavior of **2b**: a) IR and b) P-XRD initial (black) and [pH > 8.5] (red)

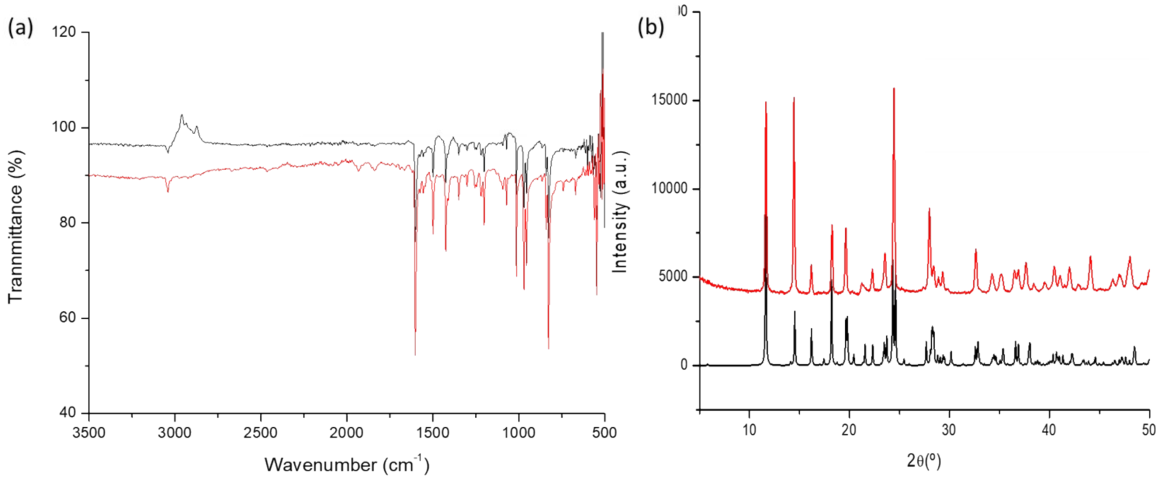


**Figure S23:** Example **2b**: a) IR and b) P-XRD initial (black) and 4.2 < pH < 8.4 (red)

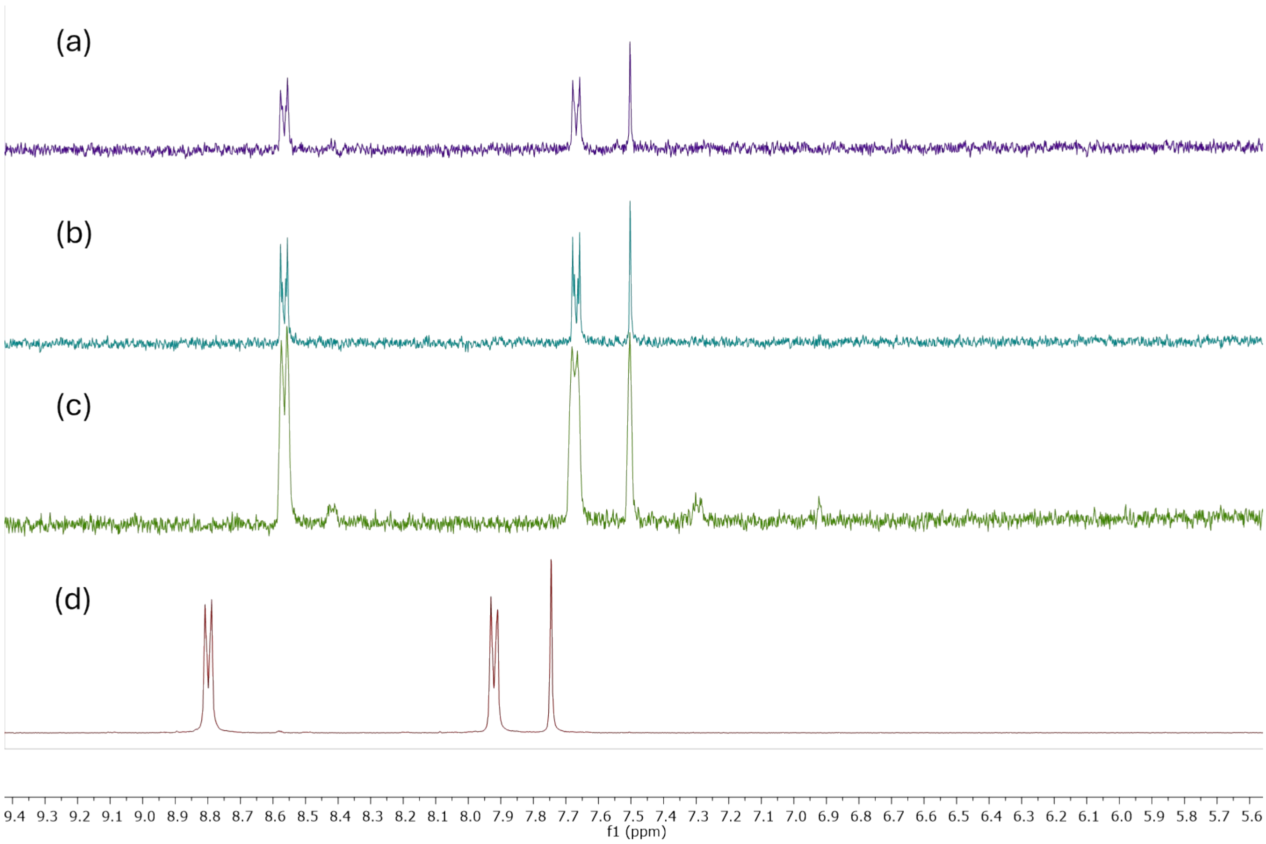


**Figure S24:** $^{1}$H-NMR study with **3b** in $D_2O$: a) $t_0$, b) dark $t_f$= 20 min, c) irradiation ($t_f$= 20 min in photoreactor 300-600 nm), and d) BPEE in $D_2O$.

**Table S8**: $^{1}$H-NMR assignment with BPEE / $[ZnI_2(BPEE)]_n$ and irradiation (hv) in $D_2O$

| Compound | (a) | (b) | (c) |
|---|---|---|---|
| BPEE | 7.75s | 7.91d | 8.82d |
| 3b | 7.45s | 7.65d | 8.55d |
| 3b + 20 min in photoreactor | 7.45 + 6.9s | 7.65 + 7.3d | 8.55 + 8.4d |

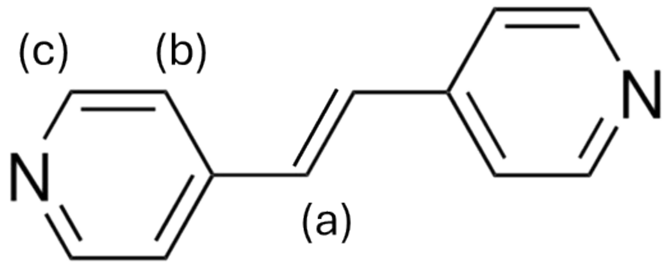


**Figure S25:** Proton assignment in the free ligand BPEE

## 9. Study of the particle size of [$Cu_2X_2$(BPEE)]$_n$

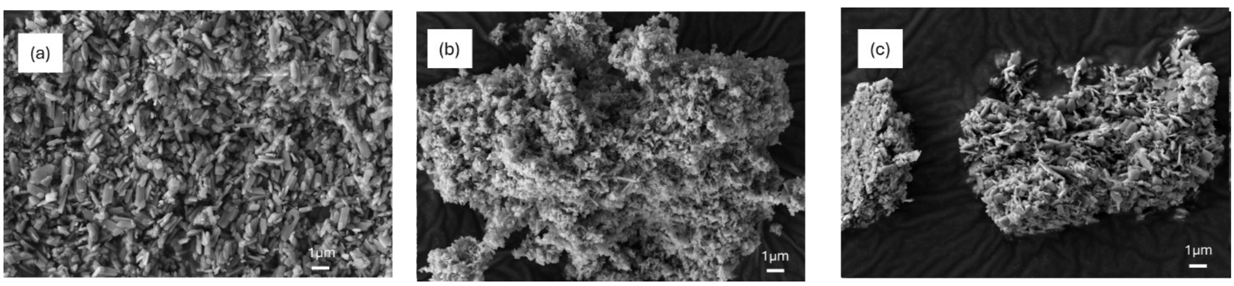


**Figure S26:** SEM of the compounds: a) **4b**, b) **5b**, and c) **6b**.

**Table S9:** Particle size with the average of **[$Cu_2X_2$(BPEE)]n** compounds over 50 particles.

| | **4b** | **5b** | **6b** |
|---|---|---|---|
| Size (µm) length | 1.1 ± 0.5 | 0.9 ± 0.5 | 1.1 ± 0.7 |
| Size (µm) width | 0.5 ± 0.2 | 0.2 ± 0.07 | 0.4 ± 0.2 |

**10. DFT calculations to explore 2D $[Cu_2X_2(BPEE)]_n$ (X= Cl (4b), Br (5b), I (6b)) theoretical band gaps and correlation with the experimental ones.**

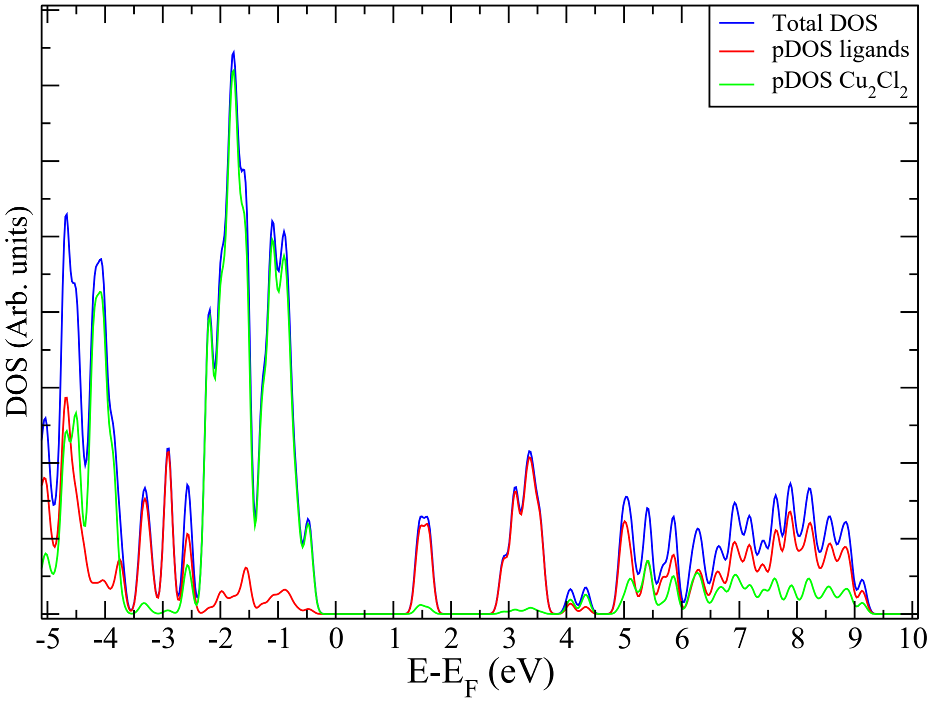


**Figure S27:** Density of States of **4b**, and projection on the atoms of ligands and the atoms of the $Cu_2Cl_2$ unit.

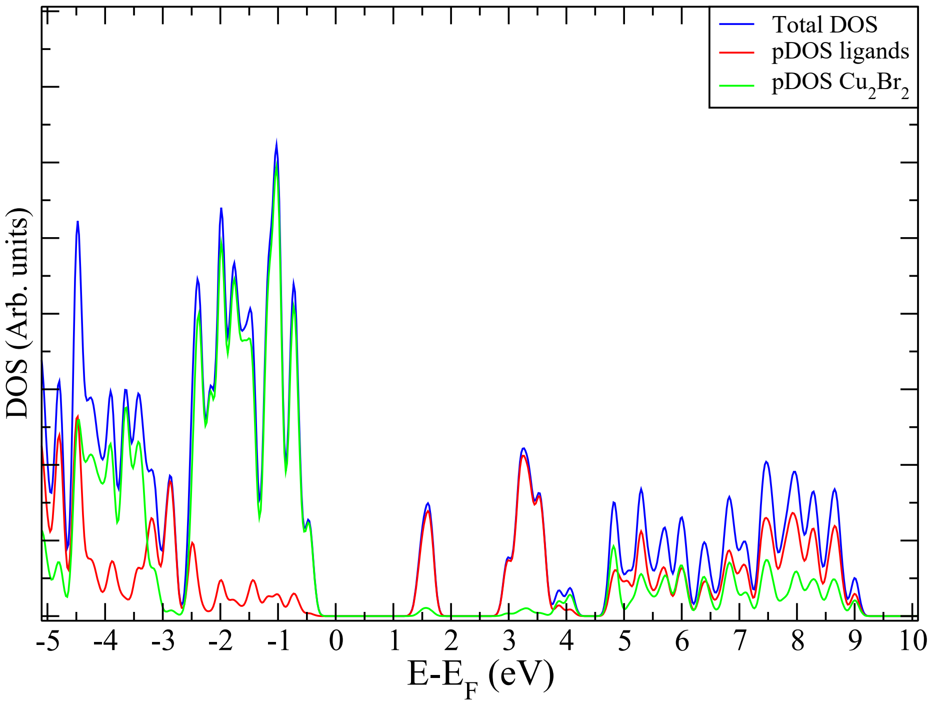


**Figure S28**: Density of States of **5b**, and projection on the atoms of ligands and the atoms of the $Cu_2Br_2$ unit.

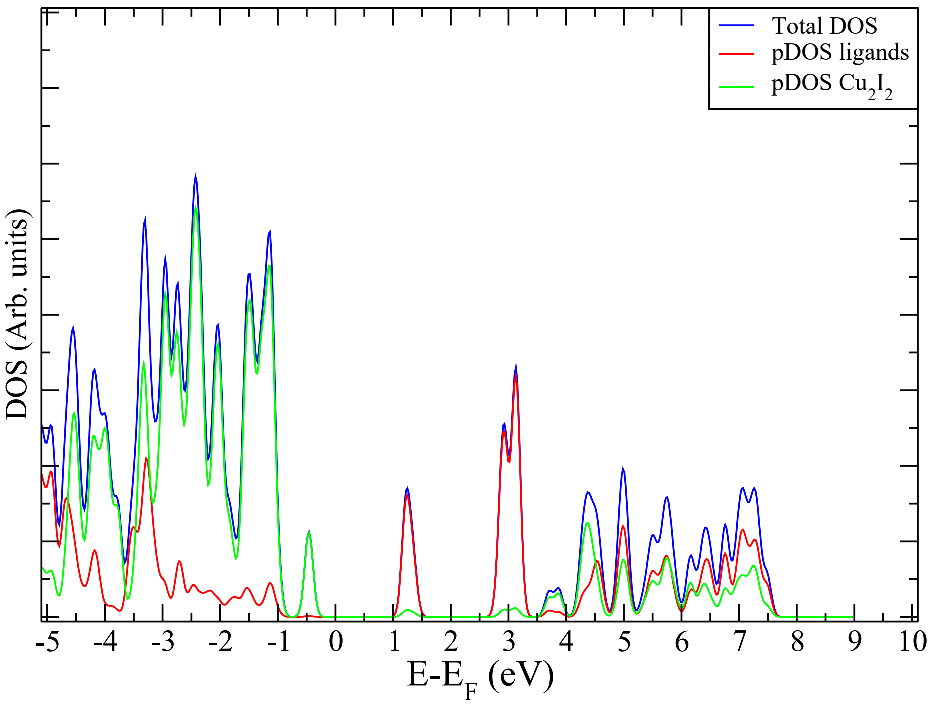


**Figure S29:** Density of States of **6b**, and projection on the atoms of ligands and the atoms of the $Cu_2I_2$ unit.

**Table S10:** Atomic charges of the Cu, the halogen, and the nitrogen on the $[Cu_2X_2(BPEE)]_n$ compounds.

| Atom | **4b** | **5b** | **6b** |
|---|---|---|---|
| Cu | 0.62 | 0.54 | 0.44 |
| X | -0.67 | -0.59 | -0.46 |
| N | -1.27 | -1.27 | -1.26 |

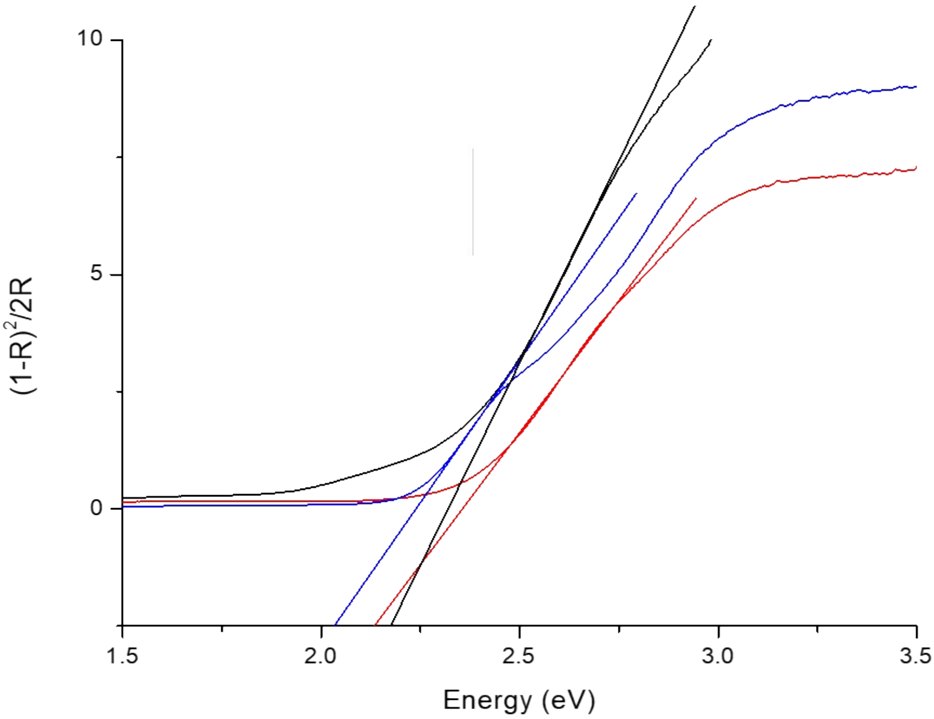


**Figure S30:** Experimental band gap value by diffuse reflectance of **4b** (black), **5b**, (red), and **6b** (blue).

## 11. Water and thermal stability of $[Cu_2X_2(BPEE)]_n$ (X=Cl (4b), Br (5b), and I (6b)) compounds.

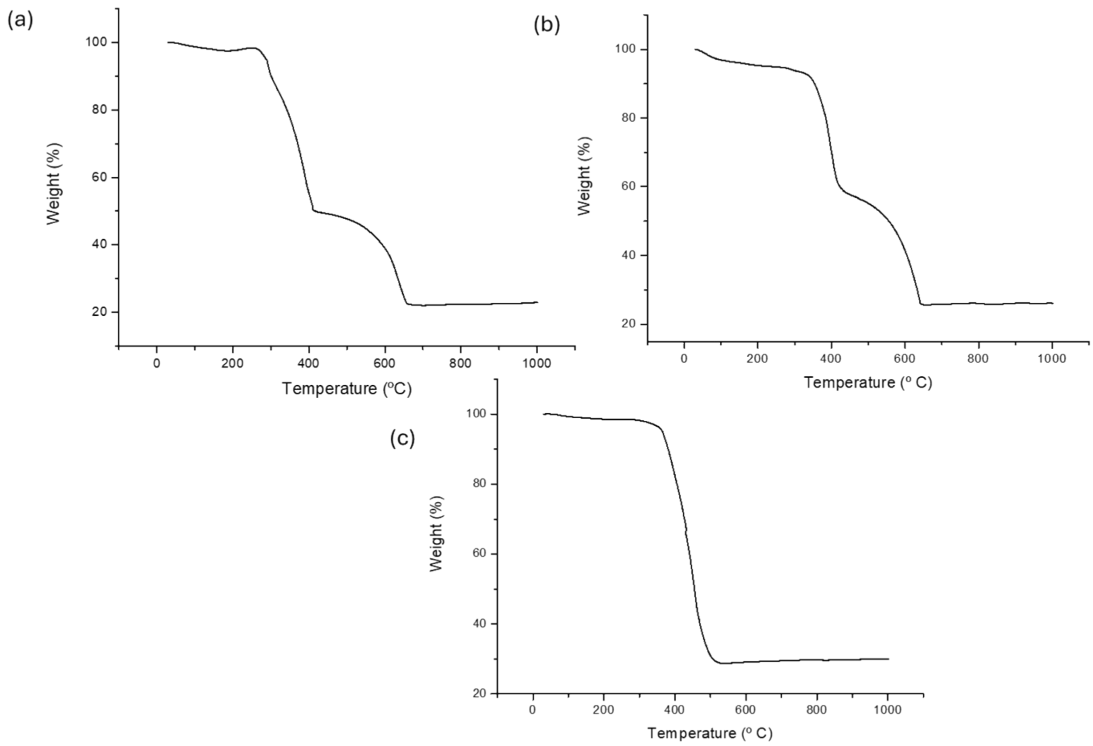


**Figure S31.** Thermogravimetric analysis (TGA) of the compounds: a) **4b**, b) **5b**, and c) **6b.**

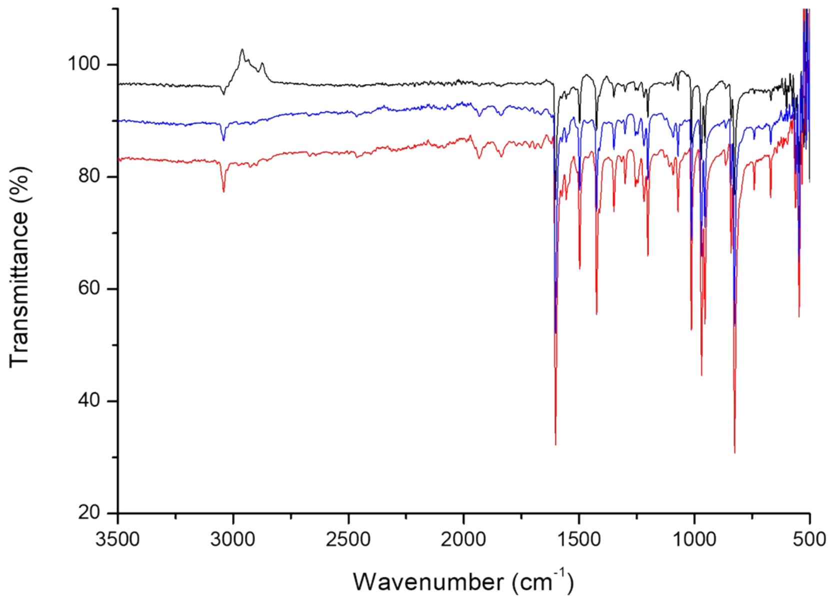


**Figure S32:** IR of $[Cu_2I_2(BPEE)]_n$ (**6b**) (black), between 2<pH<7 (red), and between 7<pH<11 (blue).

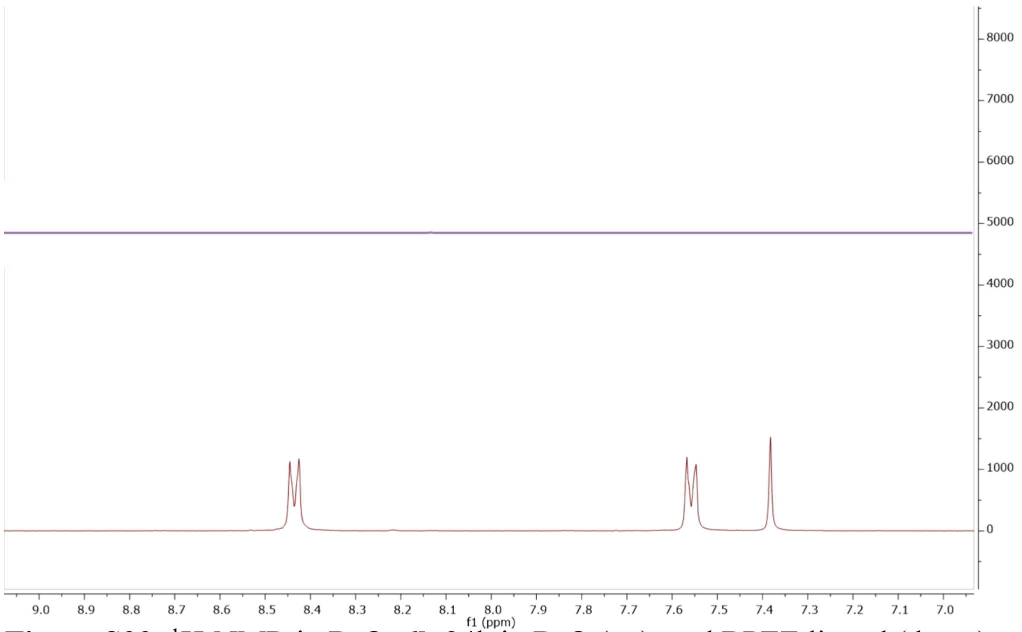


**Figure S33**: $^1$H-NMR in $D_2O$: **6b** 24h in $D_2O$ (up), and BPEE ligand (down).

**12. Study of the photocatalytic efficiency of $[Cu_2X_2(BPEE)]_n$ in the degradation of Methyl blue (MB), Methyl orange (MO), and Tartrazine (Trz).**

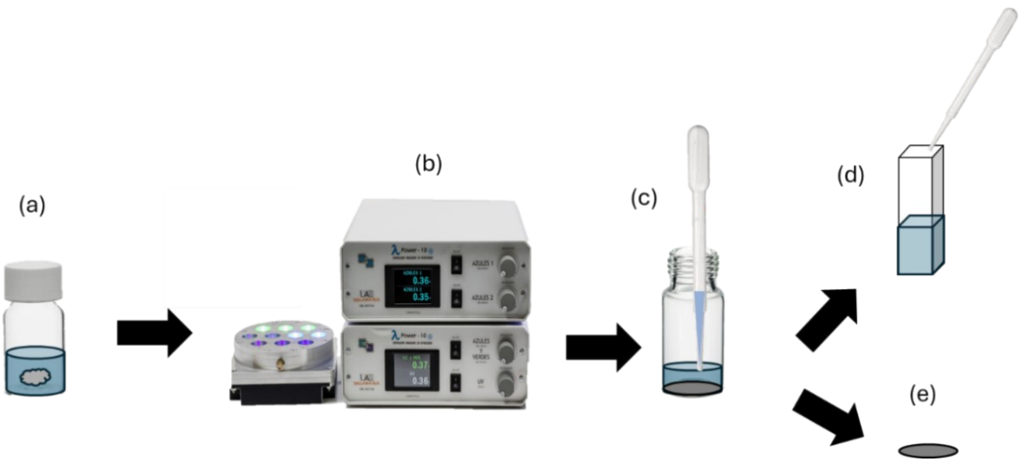


**Figure S34:** Degradation process of dyes with the compounds in the photoreactor: a) 2 mg of catalyst compound is mixed with a $10^{-5}$M organic dye aqueous solution, b) the vial is introduced into the white light photoreactor (300-600 nm) under agitation, c) the degraded dye is separated from the catalyst, d) absorbance loss of dyes by UV-vis is studied, and e) the catalyst is characterized to confirm that it maintains the structure and acts as a heterogeneous catalyst.

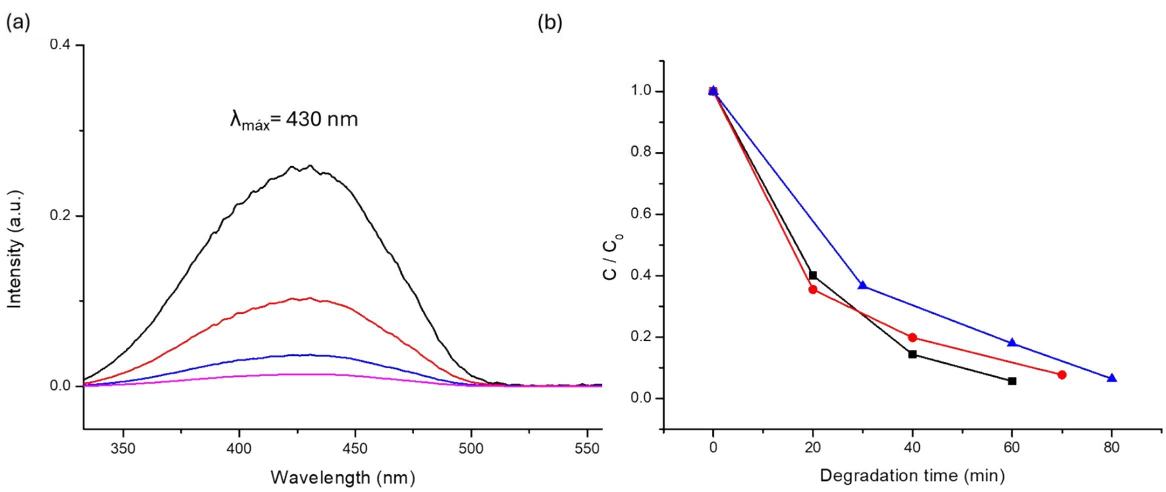


**Figure S35:** MO dye degradation: a) UV-vis degradation from 0 to 60 min for **6b** and b) plots of MO absorbance intensity loss as a function of exposure time under photoreactor, **6b** (black), **5b** (red), **4b** (blue).

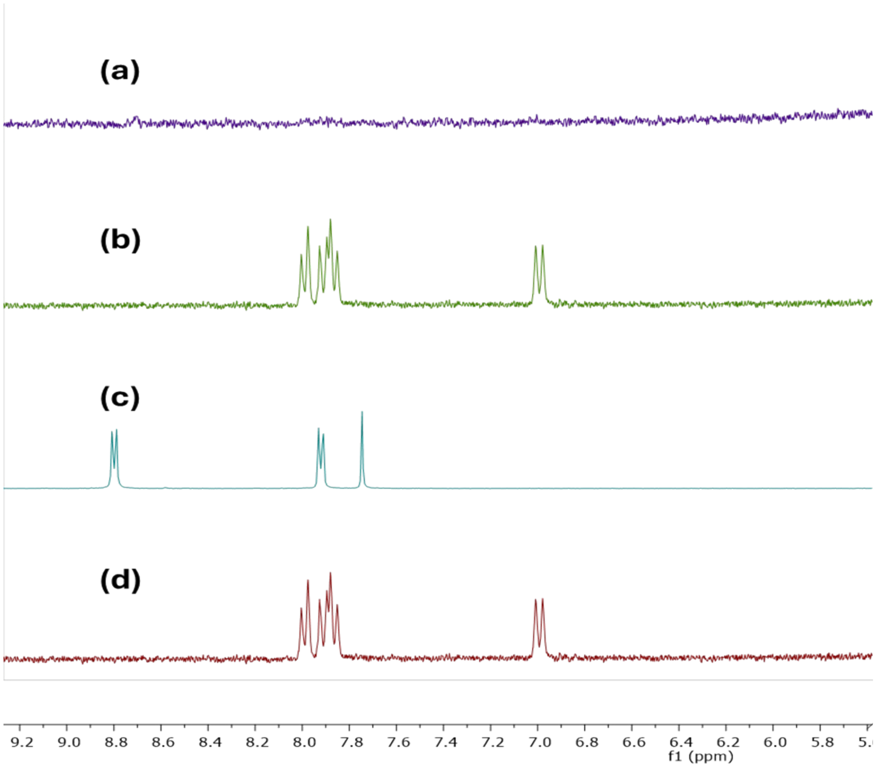


**Figure S36**: [1]H-NMR study with $[Cu_2I_2(BPEE)]_n$ (**6b**) and MO $10^{-3}$ M in $D_2O$: a) 6b+MO ($t_f$ 60 min), b) 6b+MO ($t_0$). c and d) BPEE and MO, after 60 min in $D_2O$ respectively.

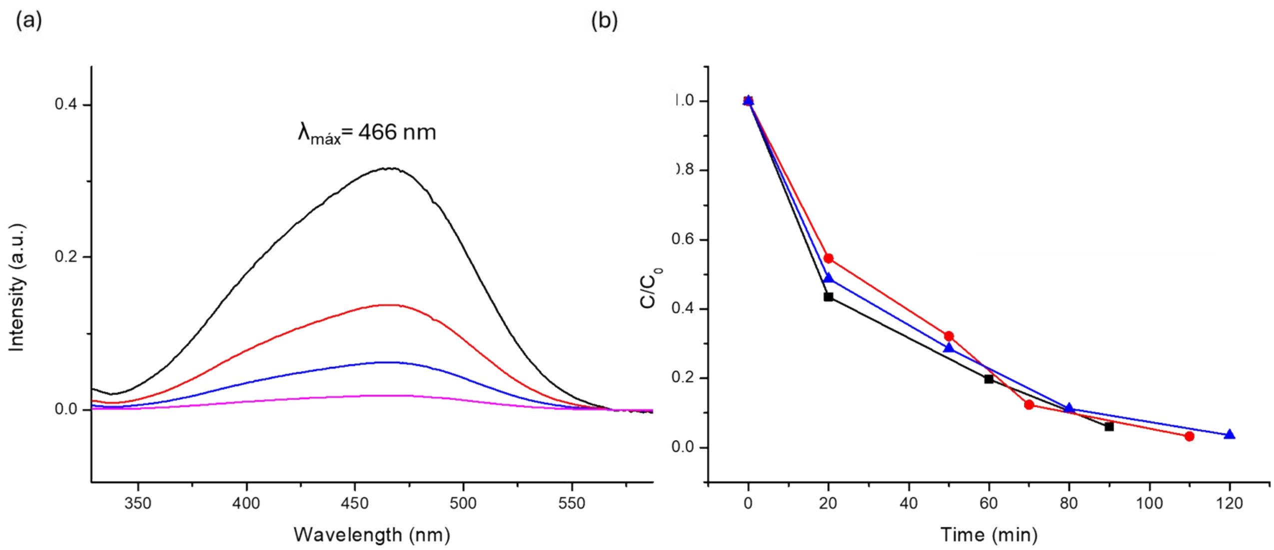


**Figure S37:** Trz dye degradation: a) UV-vis degradation from 0 to 90 min for $[Cu_2I_2(BPEE)]_n$, and b) plots of Trz absorbance intensity loss as a function of exposure time under photoreactor. $[Cu_2I_2(BPEE)]_n$ (black), $[Cu_2Br_2(BPEE)]_n$ (red), and $[Cu_2Cl_2(BPEE)]_n$ (blue).

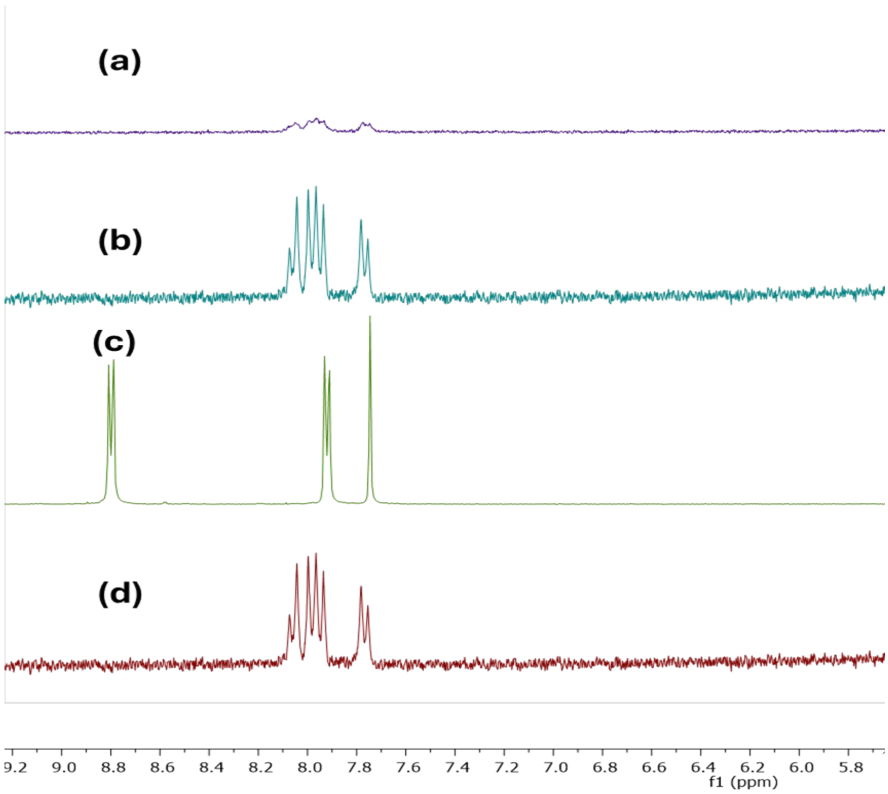


**Figure S38:** $^{1}$H-NMR study with $[Cu_2I_2(BPEE)]_n$ and Trz $10^{-3}$ M in $D_2O$: a) 6b+Trz ($t_f$), b) Trz ($t_0$), c and d) BPEE and Trz, after 60 min in $D_2O$ respectively.

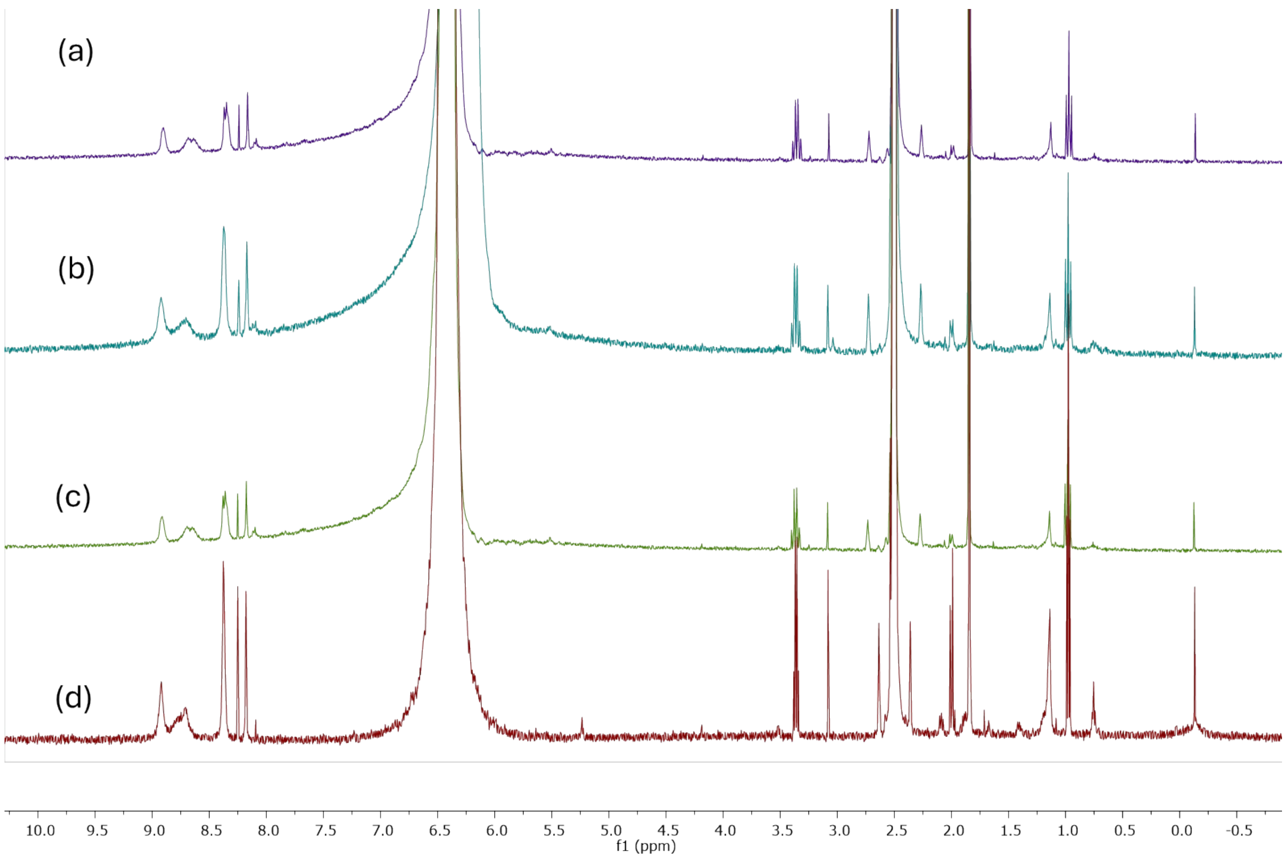

**Figure S39:** [1]H-NMR study with $[Cu_2I_2(BPEE)]_n$ *(***6b***)* post degradation of the dyes dissolved in DMSO-$d_6$ (+ two drops of DCl). After the degradation of MB (a), Trz (b), and MO (c). Initial $[Cu_2I_2(BPEE)]_n$ dissolved in DMSO-$d_6$ (+ two drops of DCl) (d).

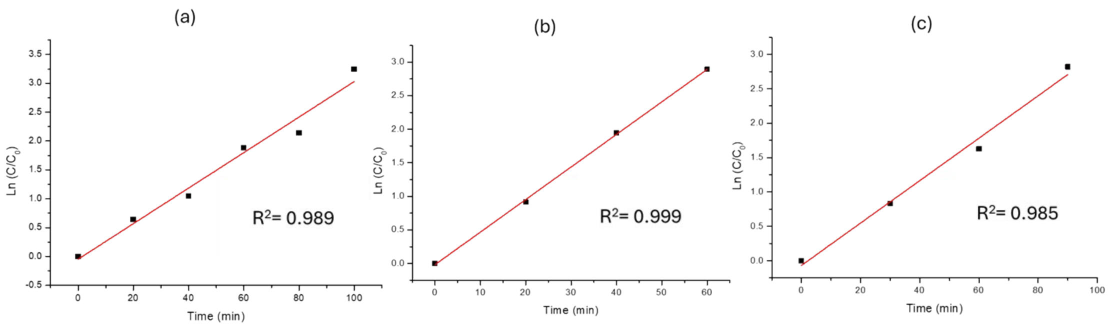


**Figure S40**. Reaction kinetics of compound $[Cu_2I_2(BPEE)]_n$: order 1 in a) MB, b) MO, and c) Trz.

## 13. Study of the mechanism of photocatalysis via ROS species traps in CPs

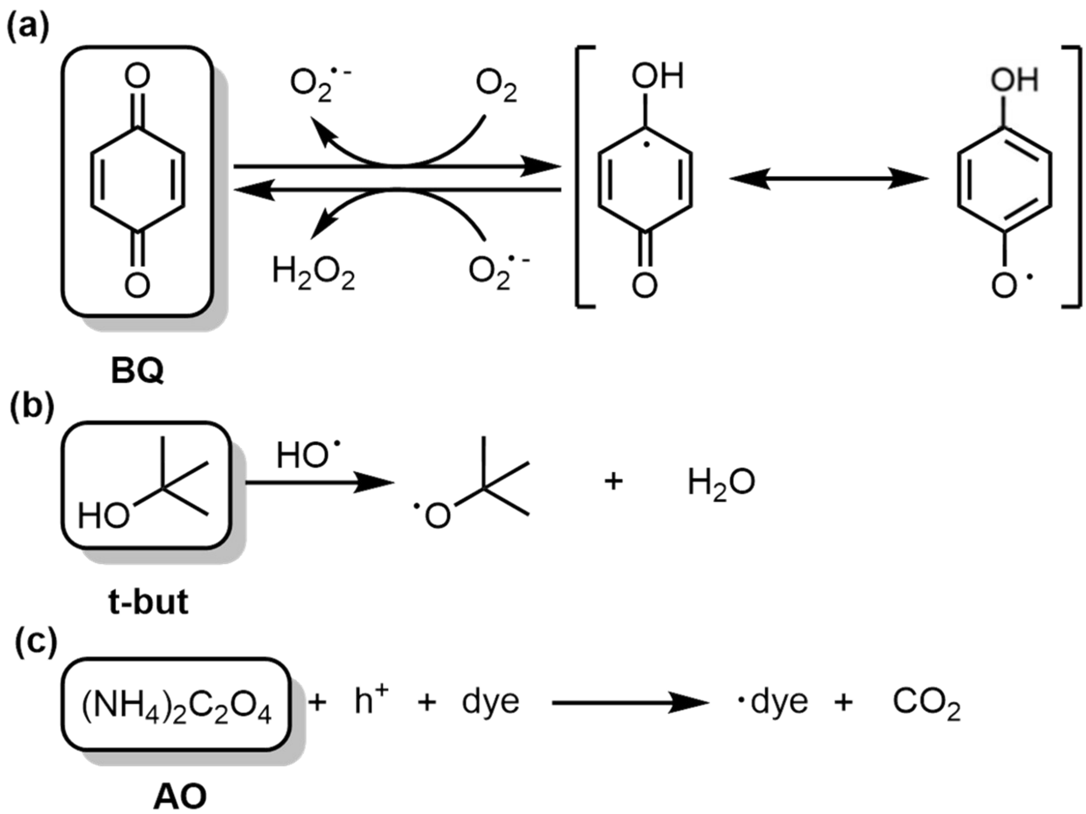


**Figure S41**: Trappers: a) benzoquinone (BQ) **·OH**, tert-butanol (t-but) **$·O_2^-$** and c) ammonium oxalate (AO) (**$h^+$**)

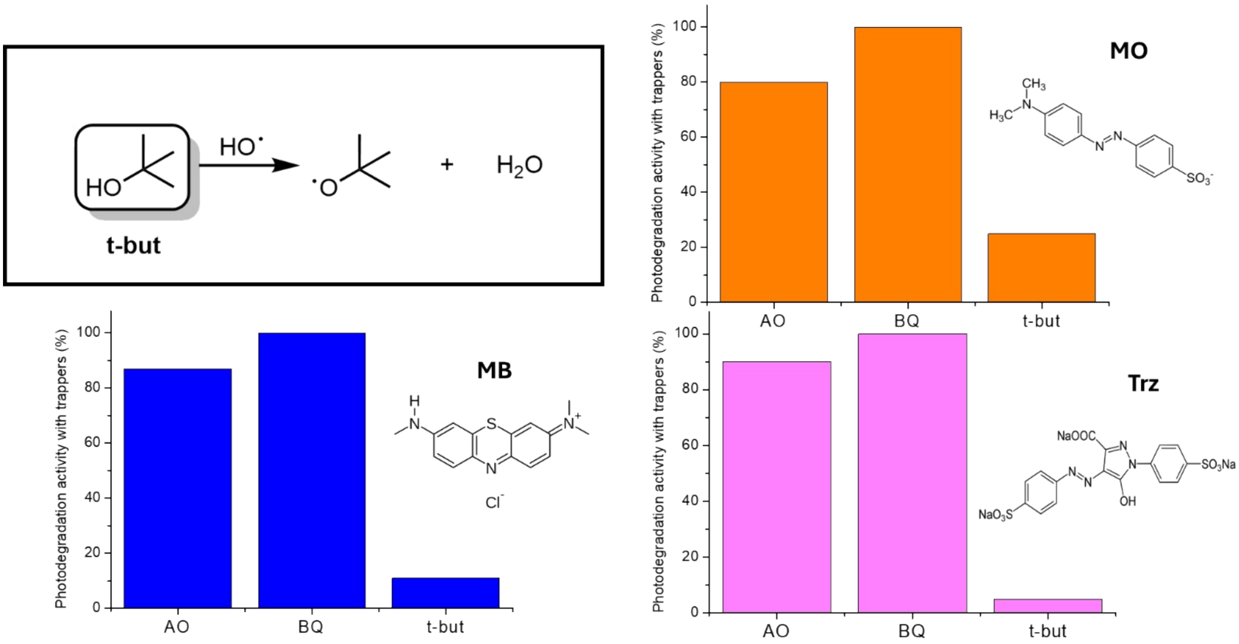


**Figure S42**: Photocatalytic activity of dyes $10^{-5}$M with $[Cu_2X_2(BPEE)]_n$ hole/radical trapper agents after. The degradation of dyes is via radical (**·OH**).

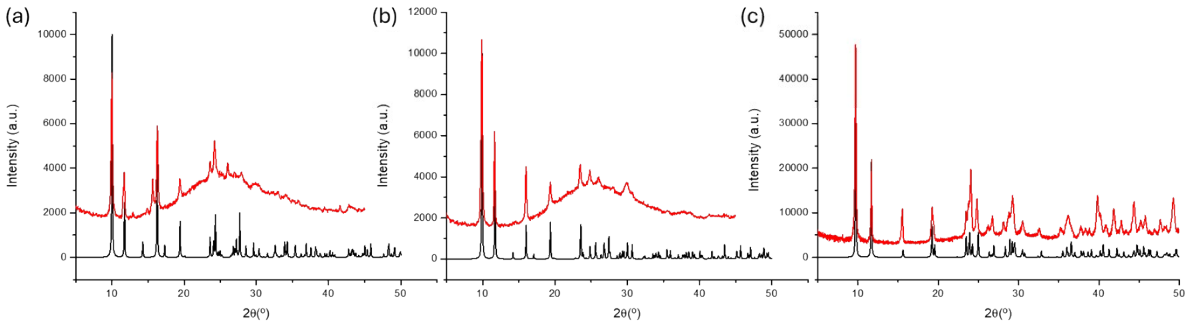


**Figure S43:** P-XRD of compounds (a) **4b**, (b) **5b** and (c) **6b**. P-XRD Simulated (black) and after the maximum number of cycles of dye (MO) degradation (red).